M.Tech (Power Electronics and Systems)

RAHUL

2025

Sliding Mode-Controlled Quadratic Boost Converter with Integrated PI for Robust Voltage Regulation.

A DISSERTATION

SUBMITTED IN PARTIAL FULFILLMENT OF THE REQUIREMENTS

FOR THE AWARD OF THE DEGREE

OF

MASTER OF TECHNOLOGY

IN

POWER ELECTRONICS AND SYSTEMS

Submitted by:

RAHUL

2K23/PES/11

Under the supervision of

PROF.SUDARSHAN KUMAR BABU VALLURU

(Professor, EED, DTU)

DEPARTMENT OF ELECTRICAL ENGINEERING

DELHI TECHNOLOGICAL UNIVERSITY

(Formerly Delhi College of Engineering)

Bawana Road, Delhi-110042

MAY 2025

DEPARTMENT OF ELECTRICAL ENGINEERING

DELHI TECHNOLOGICAL UNIVERSITY

(Formerly Delhi College of Engineering)

Bawana Road, Delhi-110042

CANDIDATE'S DECLARATION

I, Rahul, Roll No. 2K23/PES/11 student of MTech (Power Electronics & Systems), hereby declare that the project Dissertation titled "**Sliding Mode-Controlled Quadratic Boost Converter with Integrated PI for Robust Voltage Regulation**" which is submitted by me to the Department of Electrical Engineering, Delhi Technological university, Delhi in partial fulfilment of the requirement for the award of the degree of Master of Technology, is original and not copied from any source without proper citation. This work has not previously formed the basis for the award of any Degree, Diploma Associateship, Fellowship, or other similar title or recognition.

Place: Delhi **(Rahul)**

Date: 24th May 2025

DEPARTMENT OF ELECTRICAL ENGINEERING

DELHI TECHNOLOGICAL UNIVERSITY

(Formerly Delhi College of Engineering)

Bawana Road, Delhi-110042

CERTIFICATE

I hereby certify that the project Dissertation titled "**Sliding Mode-Controlled Quadratic Boost Converter with Integrated PI for Robust Voltage Regulation**" which is Submitted by Rahul, Roll No. 2K23/PES/11, Department of Electrical Engineering, Delhi Technological University, Delhi in partial fulfilment of the requirement for the award of the degree of Master of Technology, is a record of the project work carried out by the student under my supervision. To the best of my knowledge, this work has not been submitted in part or full for any Degree or Diploma to this University or elsewhere.

Place: Delhi

Date: 24th May 2025

PROF.SUDARSHAN KUMAR
BABU VALLURU
(SUPERVISOR)

DEPARTMENT OF ELECTRICAL ENGINEERING

DELHI TECHNOLOGICAL UNIVERSITY

(Formerly Delhi College of Engineering)

Bawana Road, Delhi-110042

ACKNOWLEDGEMENT

I would like to express my gratitude towards all the people who have contributed their precious time and effort to help me without whom it would not have been possible for me to understand and complete the project. I would like to thank **Prof. Sudarshan Kumar Babu Valluru, DTU Delhi, Department of Electrical Engineering**, my Project Supervisor, for supporting, motivating, and encouraging me throughout this work carried out. His readiness for consultation always, his educative comments, and his concern and assistance even with practical things have been invaluable.

Besides my supervisor, I would like to thank **Mr. Dipak Prasad** (Ph.D. scholar) and all the Ph.D. scholars of Control System LAB for helping me wherever required and providing me with continuous motivation during my research.

Finally, I must express my very profound gratitude to my parents, seniors, and my friends for providing me with unfailing support and continuous encouragement throughout the research work.

Date: 24th May 2025 **Rahul**

M.tech (Power Electronics & Systems)

Roll No. 2K23/PES/11

ABSTRACT

This thesis offers an extensive analysis of a sliding mode-controlled quadratic boost converter (QBC) combined with proportional-integral (PI) compensation to attain resilient voltage regulation in renewable energy and electric car applications. The study focuses on the essential requirement for high-gain DC-DC converters that can effectively convert low input voltages to elevated output levels while ensuring stability over fluctuating load circumstances.

The suggested converter topology attains a quadratic voltage gain of $V_{out}=V_{in}(1-D)^2$, facilitating 12V-to-48V conversion at a moderate duty cycle, hence substantially diminishing component stress relative to traditional boost converters. A unique two-loop hybrid control technique is devised, incorporating an inner sliding mode controller for accurate inductor current regulation and an outside PI controller for output voltage tracking. This setup guarantees swift disturbance rejection during load fluctuations (25-75% load steps) while keeping output voltage deviation under 2%. The study utilizes state-space averaging methods to create precise dynamic models and get transfer functions essential for controller design. Comprehensive simulations confirm the converter's efficacy, exhibiting output ripple below 5%, 93% efficiency at full load, and enhanced transient response relative to traditional control techniques. The project encompasses comprehensive design approaches for inductors and capacitors functioning at a switching frequency of 50kHz.

Experimental validation substantiates the converter's resilience to input voltage fluctuations (12V-30V) and load perturbations, rendering it appropriate for photovoltaic systems, electric vehicle charging infrastructure, and DC microgrids. The thesis offers substantial progress in high-gain converter topologies and resilient control mechanisms, establishing a basis for future sustainable energy systems.

TABLE OF CONTENTS

LIST OF FIGURES

LIST OF TABLES

LIST OF ABBREVIATIONS

QBC	Quadratic Boost Converter
SMC	Sliding Mode Control
PV	Photovoltaic
EV	Electric Vehicle
PWM	Pulse Width Modulation
EMI	Electromagnetic Interference
ESR	Equivalent Series Resistances

CHAPTER 1

INTRODUCTION

1.1. Overview

An increasing global emphasis on renewable energy and sustainable power systems has driven up demand for efficient power conversion technologies. Photovoltaic (PV) systems, fuel cells, and other renewable energy sources often produce low DC voltages that must be increased to higher levels to accommodate loads or grid interface. Conventional boost converters tend to be used for this purpose, but their voltage gain is fundamentally bound by the duty cycle and pushing them to high gains frequently results in large switching losses, higher component stress, and reduced efficiency. These issues encourage the development of new converter topologies which are capable of attaining significant voltage gain without sacrificing efficiency and reliability. Modern technologies rely largely on power electronic converters to efficiently transform energy for a variety of applications. In the context of electric vehicles, these devices are critical: they convert direct current stored in high-voltage batteries into alternating current to power the drive motors, allowing for precise control of the vehicle's speed and torque. Inverters provide reverse conversion during regenerative breaking, transferring energy from the motors to the battery as direct current. In order to ensure optimal energy distribution and use, EVs' DC-DC converters are also in charge of lowering the high battery voltage to levels appropriate for auxiliary systems like climate control, lighting, and cabin electronics. Portable electronics such as smartphones and laptops rely on DC-DC converters to regulate fluctuating battery voltages, ensuring stable power delivery to sensitive components. For example, buck converters lower voltages for processors, while boost converters maintain screen brightness as batteries drain. This regulation enhances battery longevity and device reliability [1]-[5].

These converters use sophisticated semiconductor materials such as SiC and GaN to increase efficiency and thermal performance. By enhancing control techniques such as pulse-width modulation (PWM) and feedback loops, researchers continue to enhance system stability and broaden applications in new technologies like smart grids and aerospace.

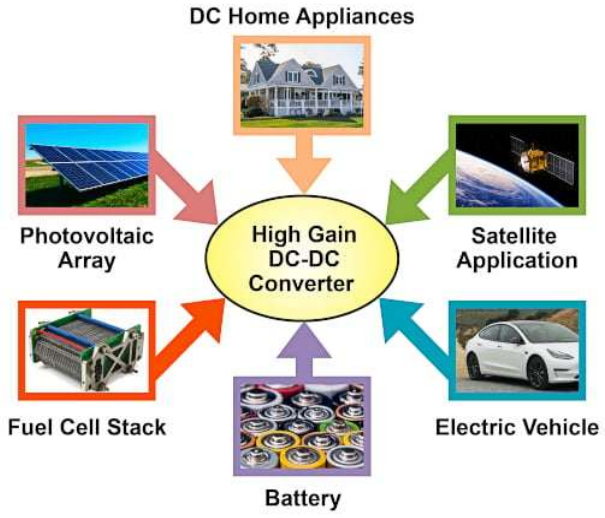

Fig1.1: Application of Power Electronics Converter Systems.

1.2 Introduction To DC-DC Converters.

In the dynamic world of electronics, the pursuit of efficient and adaptable power conversion is ongoing. DC-DC converters have transformed how power is regulated and used in modern electronics. A wide variety of applications. These converters have led to smaller, more efficient, more flexible devices, surpassing the capabilities of linear regulators [6]-[8]. Prior to the widespread adoption of DC-DC converters, linear regulators were commonly employed to regulate voltage. Linear regulators are known for their simple design and ability to give clean, stable output with low noise. However, their operating inefficiency in certain cases led to the development of other options. Linear regulators have low energy conversion efficiency due to heat dissipation during voltage regulation, especially in applications with wide input and output voltage ranges significantly. Due to this constraint, DC-DC converters were developed and widely adopted [9]-[15]. DC-DC converters use a different power conversion mechanism compared to linear regulators. They use switch-mode technology, in which high-frequency switching is utilized by power switches to

efficiently convert an input voltage to a specified output voltage. Energy is temporarily stored in inductors or capacitors and supplied at the desired output voltage, significantly decreasing waste. There are actually several benefits to switching from conventional linear regulators to DC-DC converters, chief among them being their increased efficiency. These converters are recognized for their high efficiency rates, frequently exceeding 90% [20]-[23].

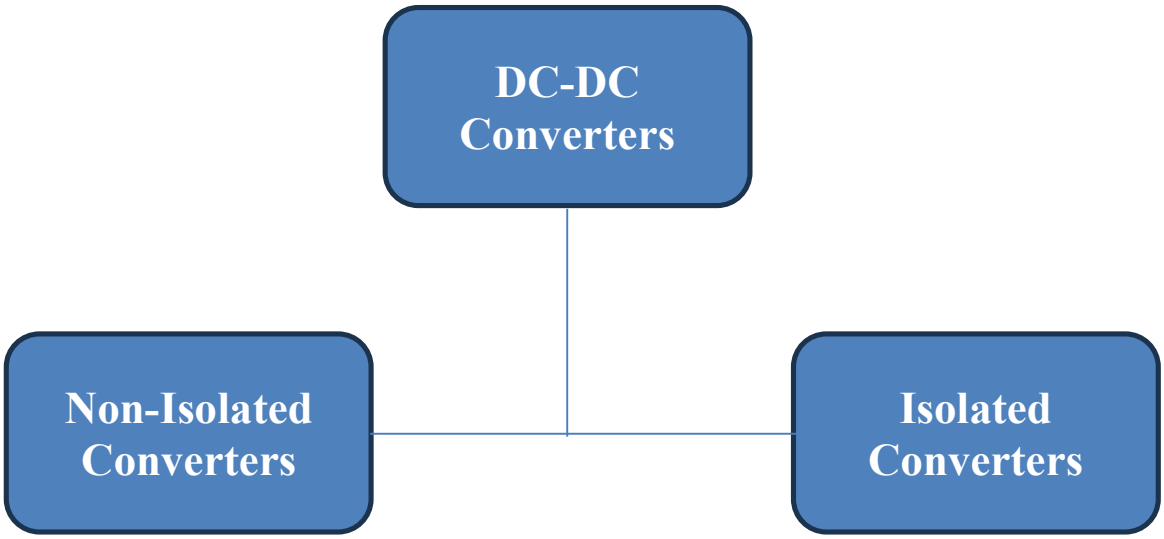

Fig1.2: Classification of DC-DC Converters.

1. **Non-Isolated Converters:** These converters allow energy to flow smoothly without an isolated hurdle, that allows for inexpensive construction and small design while offering dependable performance in a variety of surroundings. A variety of topologies are discussed, including the SEPIC, Cuk, Zeta, Boost, Buck, and Buck-boost converters.
2. **Isolated Converters:** High-frequency transformers are utilized by isolated converters to attain conditions where the input and output must be electrically isolated. They are critical to minimizing noise levels and safeguarding precious parts. These types, which are frequently employed in power electronics, include the forward converter, flyback converter, push-pull converter, half-bridge converter, and full-bridge converter.

1.3 Thesis Motivation.

DC-DC converters perform an important part in modern electronics infrastructure and have recently gained attention for their efficiency and effectiveness. The precise regulation of direct current. Converters serve a role in delivering direct current (DC) power to several circuits from a single source. We previously examined the various DC-DC converter topologies, which are tailored to specific applications through careful component selection and ratings. These may comprise input and output voltages, input current ripple, output voltage ripple, output power, and switching frequency. Particularly, the design details. This section covers both passive (inductors and capacitors) and active (semiconductor devices) components that affect converter efficiency. Converter values are essential to obtaining goals such as boosting efficiency and dependability, as well as lowering voltage and current ripples. Inductors are a critical component in converter design [24]. Their value has a direct impact on ripple current; higher inductance minimizes ripple but costs at the expense of larger size and potentially higher cost. Higher switching frequencies will reduce inductor size but bring difficulties for heat management and electromagnetic interference (EMI). In high-frequency applications, inductors' efficiency will be impacted by their resistance. To minimize losses, utilize high-quality inductors with low resistance, primarily ferrite cores. Scholarly debates often overlook non-idealities in design equations for inductors and capacitors. This research seeks to address gaps in our understanding of DC-DC converter design processes by incorporating non-idealities. Better converter designs can be predicted as a result of careful research and consideration of less-than-ideal elements such as capacitor equivalent series resistance (ESR), inductor core losses, and semiconductor switching and conduction losses. This study proposes assisting designers produce smaller, more reliable, and efficient converters by developing a comprehensive model that accounts for faults. This study's modeling of DC-DC converters demands combining accuracy with simplicity. This study aims to address the issue of modeling converter non-idealities in a way that generates more accurate and practical models, hence addressing a significant gap in existing modeling methodologies [25]– [30].

The development of better and adaptive control strategies for DC-DC converters is acknowledged as a significant research direction with the goal of maintaining output stability under a variety of changing conditions, such as input voltage variations and load variability. This study aims to determine whether employing pulse width modulation (PWM) and other cutting-edge control strategies to consistently stabilize the output voltage is feasible. Due to the inherent complexity of quadratic boost converters and other higher-order systems, this research aims to explore how non-ideal analytical methods can make the design of control strategies more straightforward. The intention is to lower computational requirements while still ensuring the control system performs effectively. By merging theoretical concepts with practical solutions, this project addresses these challenges and seeks to contribute meaningfully to the field. The ultimate goal is to enhance the design and control of DC-DC converters by narrowing the gap between theoretical models and real-world operational needs, thereby setting new benchmarks for both efficiency and effectiveness.

CHAPTER 2

DESIGN OF DC-DC CONVERTERS

2.1 Introduction

DC-DC converters are crucial because they allow for the management and modification of voltage levels in a wide variety of devices. They are important components of the electronics industry itself. In order to ensure that electronic circuits receive the voltage that is required, these converters provide the necessary voltage. The efficient operation of a wide variety of applications, ranging from portable devices such as laptops and cell phones to various forms of renewable energy systems and car electronics. DC-DC converters can be broken down into three primary topologies, each of which has its own set of characteristics and applications. Buck, boost, and buck-boost converters are all represented by these converters [31][32].

The input voltage is decreased by the buck converter, which results in a shorter output value. It is distinguished by its ability to generate a steady output current with little voltage changes, which makes it particularly efficient for applications that require a dependable power supply. This gives it a competitive advantage. On the other hand, there is a problem that needs to be taken into consideration: the input current is not continuous, which indicates that an input filter needs to be incorporated in order to ensure that the operation works smoothly [33]-[35].

On the other hand, the boost converter is responsible for increasing the output voltage by increasing the input voltage. The most remarkable aspect of this is its uninterrupted input current flow, which eliminates the demand for an input filter. On the other hand, just like the buck converter, it too has some limitations. Given that the boost topology does not have a continuous output current, this indicates that the current does not remain constant throughout the course of time. There is a requirement for a substantial amount of capacitance in order to lessen the amount of fluctuation that occurs in the output voltage [36]-[39].

The flexible buck-boost converter combines the characteristics of both buck and boost converters in order to provide output voltage levels that can be higher, lower, or equal to the input voltage. This is accomplished by mixing its attributes. In the

same way as a boost converter does, the implementation of this device provides unique challenges due to the fact that it reverses the polarity of the output voltage in relation to the input and has discontinuous currents at both the input and the output.

When compared with those topologies, the Quadratic boost converter can manage to maintain a non-inverting output voltage and avoid the complexity of designs which are based on coupled inductors or transformers. The Cuk converter is capable of providing continuous input/output currents and adjustable voltage control; however, its efficiency decreases at large gains due to switching losses and magnetic complexity. By optimizing component stress, the QBC, on the other hand, produces a higher efficiency of between 4% and 7%.

Applications relying on DC-DC converters need the ideal mix of inductance and capacitance since they depend on it. Applications relying on DC-DC converters must have the best inductance and capacitance arrangement, as many studies and academic publications show [40]-[50].

Though actual circumstances suggest differently, theoretical study and design methods typically assume the parts of these converters to be flawless. The actual components of DC-DC converters are defective and far from the ideal model. In inductors and capacitors, these flaws show as equivalent series resistances (ESRs); in MOSFETs and diodes during their operating phase, they show as extra resistances; in diodes, they show as natural forward voltage drop. Such non-ideal elements can greatly affect the performance and design details of DC-DC converters, hence complicating the creation of accurate and high-quality power supply. For example, when theoretically modelling the duty cycle formulas for a Quadratic Boost converter in continuous conduction mode (CCM) as stated in Eqn. (2.1), these real-world variances must be included to guarantee accuracy and efficiency in design.

$$\frac{V_o}{V_s} = \frac{1}{(1-D)^2} \tag{2.1}$$

Where V_o is the output voltage and V_s is the input voltage of Quadratic Boost converter.

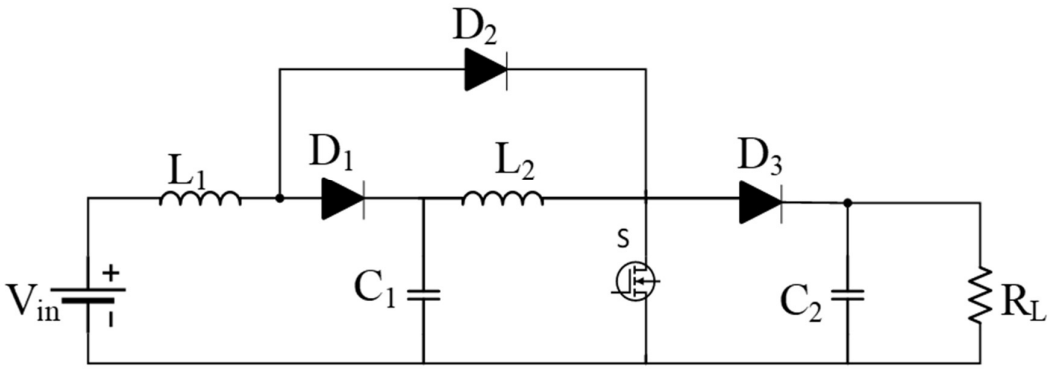

Fig 2.1: Schematic Diagram of Quadratic Boost Converter.

2.2 Analysis of Quadratic Boost DC-DC Converter

The schematic diagram of a quadratic boost DC-DC converter, as shown in Figure 2.1, exhibits a unique configuration that is utilized for the purpose of effectively regulating voltage levels. Two inductors, two capacitors, three semiconductor diodes, and a switch, which is typically a transistor, are the elements that make up this converter. By utilizing this configuration, energy is successfully transported between its input and output sides. Both inductors and capacitors, which are components that store energy, play an important part in the process of smoothing out voltage and current changes, which is necessary for ensuring that a stable output is achieved. It is the adaptability of the Quadratic boost converter that sets it apart from other converters. This versatility is evidenced by the fact that it can operate in two modes: Continuous Conduction Mode (CCM) and Discontinuous Conduction Mode (DCM). For the purposes of this investigation, the operations of the CCM are the primary focus of attention. When it comes to understanding how the converter operates under steady conditions, this mode is necessary, with a particular emphasis placed on the duty cycle (D) and the switching frequency (fs). Due to the fact that the duty cycle, which is defined as the ratio of the active time of the switch to the entire cycle time, is an essential component in the process of controlling the output of the converter, we have incorporated it into our analysis.

Mathematically,

$$D = \frac{T_{on}}{T_{on}+T_{off}} = \frac{T_{on}}{T_s} = T_{on}f_s \qquad 2.2$$

Where T_{on} is the time of interval when the MOSFET is turned ON and T_{off} is the time interval when MOSFET is turned OFF.

From Eqn. (2.2), We get,

$$T_{on} = DT_s \text{ (When MOSFET is Turned ON)} \qquad 2.3$$

$$T_{off} = (1-D)T_s \text{(When MOSFET is Turned OFF)} \qquad 2.4$$

Quadratic Boost converter is controlled by MOSFET switching mechanisms. In CCM mode it has two switching mode (a) When the MOSFET is ON and the Diode is turned OFF, or (b) When the MOSFET is turned OFF and the Diode Conducts.

2.3 Mode I Operation ($0 < t < DT_s$)

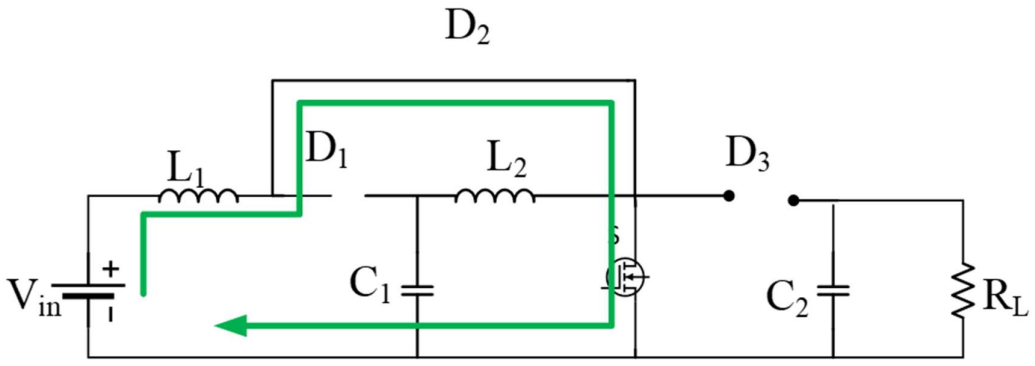

Fig 2.2: Schematic Diagram of Quadratic Boost during MODE I Operation.

When referring to a Quadratic Boost DC-DC converter, the phase known as Mode 1 is the phase in which the MOSFET is activated and the diodes D1 and D3 are non-conducting, while the diode D2 is conducting. During the process of turning on the MOSFET in Mode 1, the current travels through an inductor, L1, the MOSFET, and finally to the ground. The voltage that is placed across inductor L1 causes the current that flows through it to grow in a linear fashion with the passage of time.

More energy is stored in inductor L1 as a result of the energy it receives from the input voltage source. Due to the fact that it is storing energy from the previous cycle, the capacitor C2 begins to discharge through the closed MOSFET at this point in time. As a result, the voltage across C2 gets lower.

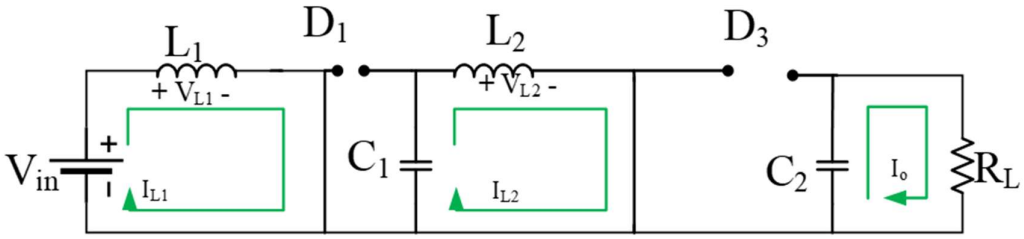

Fig 2.3: Equivalent Circuit Diagram for MODE I Operation.

Using Kirchoff's law of voltage and current, the voltage across the inductor L1 and L2, the current across the capacitor C1 and C2, and the output voltage may be calculated as follows:

$$V_{L_1,on} = L_1 \frac{di_{L_1}}{dt} = V_s \quad 2.5$$

$$V_{L_2,on} = L_2 \frac{di_{L_2}}{dt} = V_c \quad 2.6$$

$$i_{C_1,on} = C_1 \frac{dV_{C_1}}{dt} = i_{L_2} \quad 2.7$$

$$i_{C_2,on} = C_2 \frac{dV_{C_2}}{dt} = -\frac{V_o}{R_o} \quad 2.8$$

$$V_o = V_{C_2} \quad 2.9$$

2.4 Mode II Operation ($DT_s < t < (1-D)T_s$)

Changes occur in the dynamics of the system during the second stage of the Quadratic Boost converter, which occurs when the MOSFET is turned off. It is observed that the diodes D1 and D3 begin to conduct, however the diode D2 fails

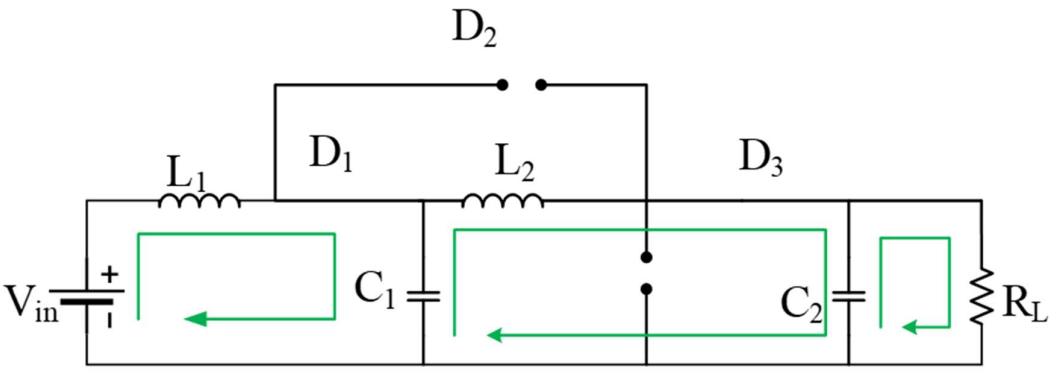

Fig 2.4: Schematic Diagram of Quadratic Boost during MODE II Operation.

to conduct. Currently, the inductor L1, which had been accumulating current, is now forcing that current through diodes, which begin to conduct as a result of the MOSFET's lack of activity. This current then continues on to charge capacitor C1, and the energy that was stored in L2 is transmitted to the output capacitor C2 as well as the load. The two different modes of functioning are depicted in Figure 2.

Using Kirchoff's law of voltage and current, the voltage across the inductor L1 and L2, the current across the capacitor C1 and C2, and the output voltage may be calculated as follows:

$$V_{L_1,off} = L_1 \frac{di_{L_1}}{dt} = V_s - V_{C_1} \qquad 2.10$$

$$V_{L_2,off} = L_2 \frac{di_{L_2}}{dt} = V_{C_1} - V_{C_2} \quad 2.11$$

$$i_{C_1,off} = C_1 \frac{dV_{C_1}}{dt} = i_{L_1} - i_{L_2} \quad 2.12$$

$$i_{C_2,0ff} = C_2 \frac{dV_{C_2}}{dt} = i_{L_2} - \frac{V_{C_2}}{R_o} \quad 2.13$$

$$V_O = V_{C_2} \quad 2.14$$

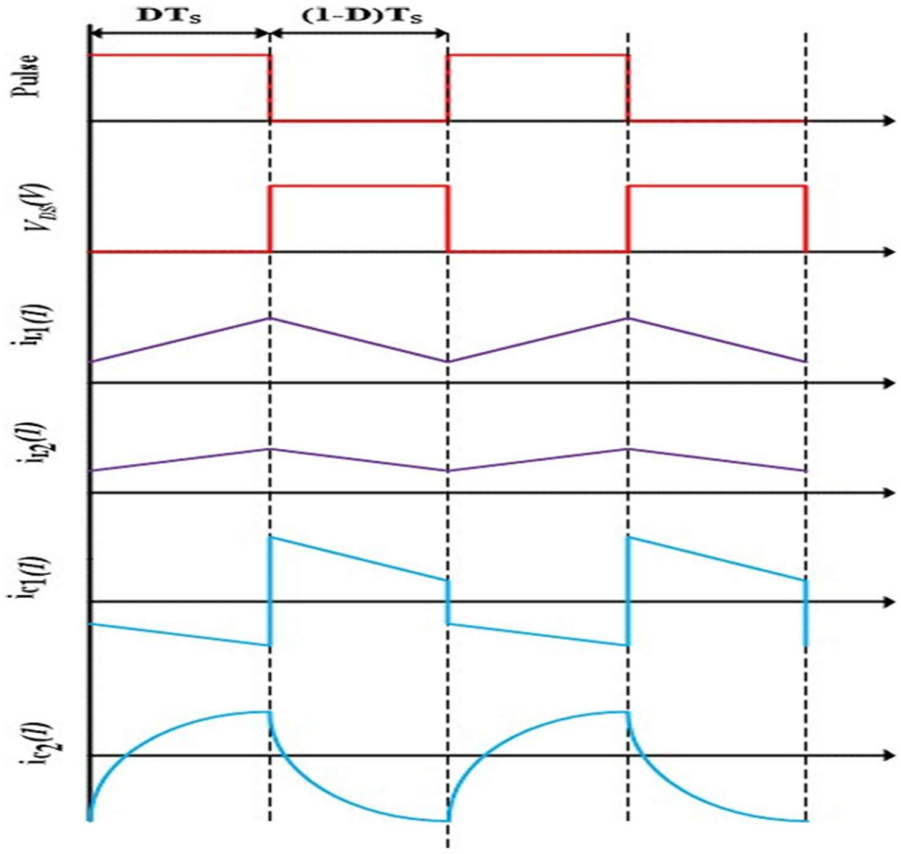

Fig 2.5: Switching waveform for Quadratic Boost converter.

2.5 Steady State Analysis.

In the context of steady-state analysis, the mean value of a current and voltage variable, denoted as x can be described as follows:

$$X = \frac{1}{T}\int_0^T x(t)dt = \frac{1}{T}\int_0^{DT} x_{on}(t)dt + \frac{1}{T}\int_{DT}^T x_{off}(t)dt \quad 2.15$$

Where x_{on} and x_{off} denotes the variable x(t) when switch is on and off respectively.

According to the principle of volt-second balance for an inductor, over a full cycle of a switched-mode power supply, the cumulative voltage applied to an inductor equals zero i.e,

$$V_L = \frac{1}{T}\int_0^T v_L(t)dt = \frac{1}{T}\int_0^{DT} v_{L,on}(t)dt + \frac{1}{T}\int_{DT}^T v_{L,off}(t)dt = 0 \quad 2.16$$

Similarly, as per the Ampere-Second balance for a capacitor, over a complete switching cycle, the net charge transferred to and from a capacitor equals zero, signifying a state of dynamic equilibrium. This is given by:

$$I_C = \frac{1}{T}\int_0^T i_c(t)dt = \frac{1}{T}\int_0^{DT} i_{c,on}(t)dt + \frac{1}{T}\int_{DT}^T i_{c,off}(t)dt \quad 2.17$$

Also, the average output voltage of the Quadratic Boost converter is given by:

$$V_o = \frac{1}{T}\int_0^T v_o(t)dt = \frac{1}{T}\int_0^{DT} v_{o,on}(t)dt + \frac{1}{T}\int_{DT}^T v_{o,off}(t)dt \quad 2.11$$

2.6 Expression for output Voltage.

The output voltage of Quadratic Boost Converter can be determined by applying volt-second balance to the inductor L1. By substituting equation 2.5 and equation 2.10 into equation 2.16, we obtain:

$$\frac{1}{T}\int_0^{DT} V_S dt + \frac{1}{T}\int_{DT}^{T} (V_S - V_{C_1}) dt = 0 \qquad 2.12$$

On simplifying the eq.2.19 we get,

$$V_S D + (1-D)\left(V_s - V_{C_1}\right) = 0 \qquad 2.3$$

$$V_S - (1-D)V_{C1} \qquad 2.21$$

Similarly, the average Voltage of capacitor C1 can be calculated by applying KVL from voltage source to the output voltage,

$$V_{C1} = V_{C2} - DV_{C2} \qquad 2.22$$

Substituting the value from eq(2.21) to eq.(2.22), we get

$$\frac{V_o}{V_s} = \frac{1}{(1-D)^2} \qquad 2.23$$

Table 1.1: Specification of Quadratic Boost converter.

Parameters	**Values**
Input Voltage Vs	12V
Output Voltage Vo	48V
Load Resistance Ro	23.0.4Ω
Inductance L1	$145\mu H$
Inductance L2	$576\mu H$
Capacitor C1	$200\mu F$
Filter Capacitor C2	$47\mu F$
Switching Frequency fs	50KHz
Desired Inductor Current Ripple$\Delta i_{L1}/\Delta i_{L2}$	$10\%I_{L1}/10\%I_{L2}$
Desired Output Voltage Ripple Current Ripple$\Delta V_{C1}/\Delta V_{C2}$	$1\%V_{C1}/1\%V_{C2}$

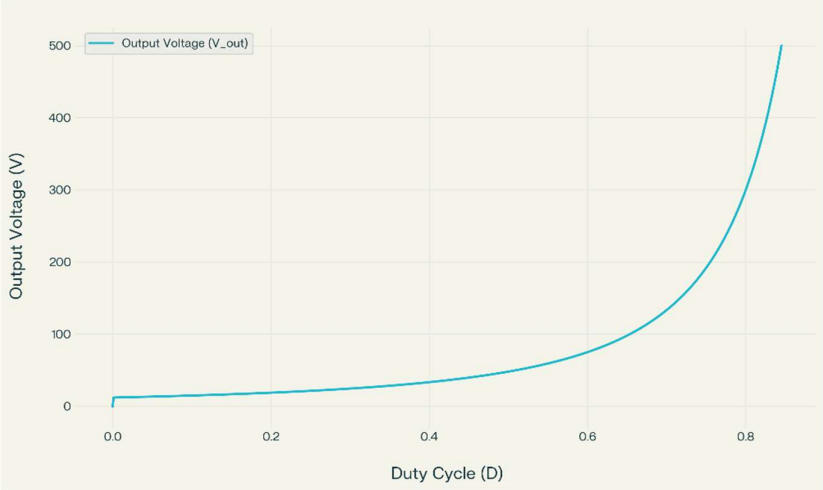

Fig 2.6: Output Voltage Variation with Duty Cycle.

2.7 Inductor Current Ripple and Inductor Design.

The design of inductors is crucial to the efficiency of DC-DC converters. It affects their efficiency, dimensions, and regulation of voltage variations. Inductors are pivotal in the storage and transfer of energy, influencing the overall performance of the converter. Consequently, prioritizing innovation in inductor design is crucial for attaining more efficient, compact, and resilient DC-DC converters.

Let Δi_{L1} and Δi_{L2} be the desired ripple in inductor current (ICR) and x_{L1} and x_{L2} be the desired inductor current ripple factor (ICRF) for both the inductors. The relationship between the ICR and ICRF is given by:

$$x_{L_1} = \frac{\Delta i_{L_1}}{I_{L_1}} \qquad 2.24$$

Similarly, $x_{L_2} = \frac{\Delta i_{L_2}}{I_{L_2}}$

Where, I_{L1} and I_{L2} are the average currents flowing through inductor L1 and L2.

Now, under steady state, using eq. (2.5), it can be written as,

$$L_1 \frac{di_{L_1}}{dt} = V_s \quad 2.25$$

By substituting the switch on duration, dt = DTs, we get,

$$L_1 = \frac{V_S * DT_s}{\Delta i_{L_1}} \quad 2.26$$

Since Ts = 1/fs, therefore eq.2.27 can be rewritten as,

$$L_1 = \frac{V_S * D}{\Delta i_{L_1} * f_s} \quad 2.27$$

Similarly for Inductor L2,

$$L_2 = \frac{V_S * D}{(1-D)\Delta i_{L_2} * f_s} \quad 2.28$$

Fig 2.7: Variation Of Inductance with Duty Cycle.

2.8 Output Voltage Ripple and Capacitor Design.

When it comes to assessing the overall efficiency and performance of the system, the capacitor is a very important component. By minimizing voltage ripples and improving power stability, a capacitor that has been constructed to its full potential ensures that energy can be transferred between circuits without any interruptions. This essential component performs the function of a buffer while simultaneously storing and releasing electrical energy. As a result, it helps to smooth out the output voltage and reduce electromagnetic interference. The design specifications of the capacitor, which include its capacity, voltage rating, and physical size, need to be meticulously tuned in order to match the exact criteria that are imposed by the converter. The fact that it makes it possible to achieve high levels of efficiency, operational dependability, and durability of the converter highlights the importance of exact capacitor design in the process of developing an optimum Quadratic Boost DC converter.

In steady state, let $\Delta V_{C1}$and ΔV_{C2} be the desired voltage ripple across the capacitors C1 and C2.

Considering the eq. (2.7), and considering the average value of inductor current i_{L2}we get,

$$Q_{C1} = C_1 \Delta V_{C1} \tag{2.29}$$

$$C_1 = \frac{I_{o.D.T_S}}{(1-D).\Delta V_{C1}} \tag{2.30}$$

$$C_1 = \frac{V_o .D}{R_o(1-D).\Delta V_{C1}.f_s} \tag{2.31}$$

Similarly for Inductor L2,

$$C_2 = \frac{V_o .D}{R_o.\Delta V_{C2}.f_s} \qquad 2.32$$

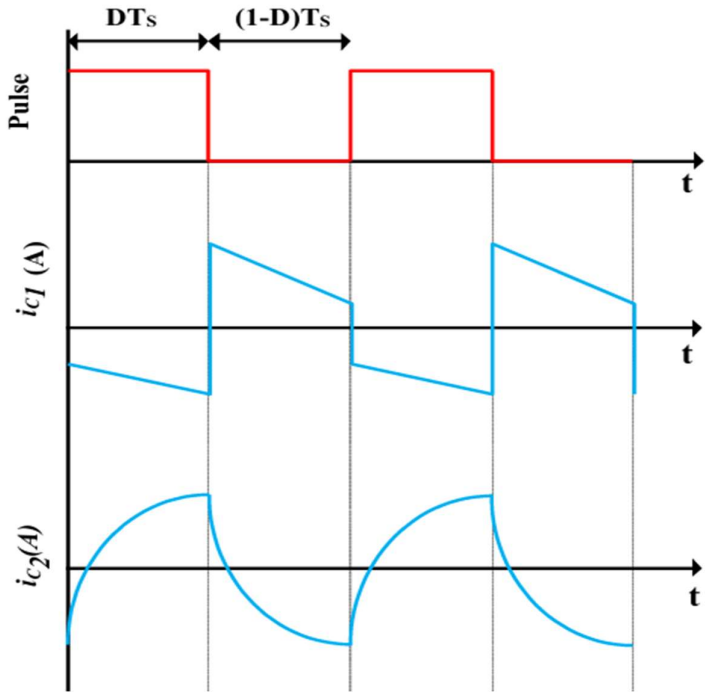

Fig 2.8: Charging and Discharging Behavior of Capacitor C1 and C2.

2.9 Result and Discussion.

The optimum Quadratic Boost converter was theoretically analyzed by simulation in MATLAB Simulink, utilizing the parameters stated in Table 2.1. The simulation sought to analyze the output voltage response under diverse scenarios. The results demonstrate that the output voltage is closely aligned with the anticipated behavior forecasted by theoretical models. As the duty cycle increased, the output voltage correspondingly increased, demonstrating a linear correlation. Conversely, a drop in the duty cycle resulted in a decrease in output voltage.

The converter, with a meticulously determined duty cycle of 0.5 in accordance with Equation 2.1, and inductance values of 0.145mH for L1 and 0.576mH for L2, was designed to convert a 12V input to a 48V output, as specified by Equation 2.2. During the simulation, the Quadratic Boost converter demonstrated exceptional

performance, maintaining a consistent and stable 48V output under open-loop conditions.

Fig 2.9: Ripple Voltage Variation with Switching Frequency for C1 and C2.

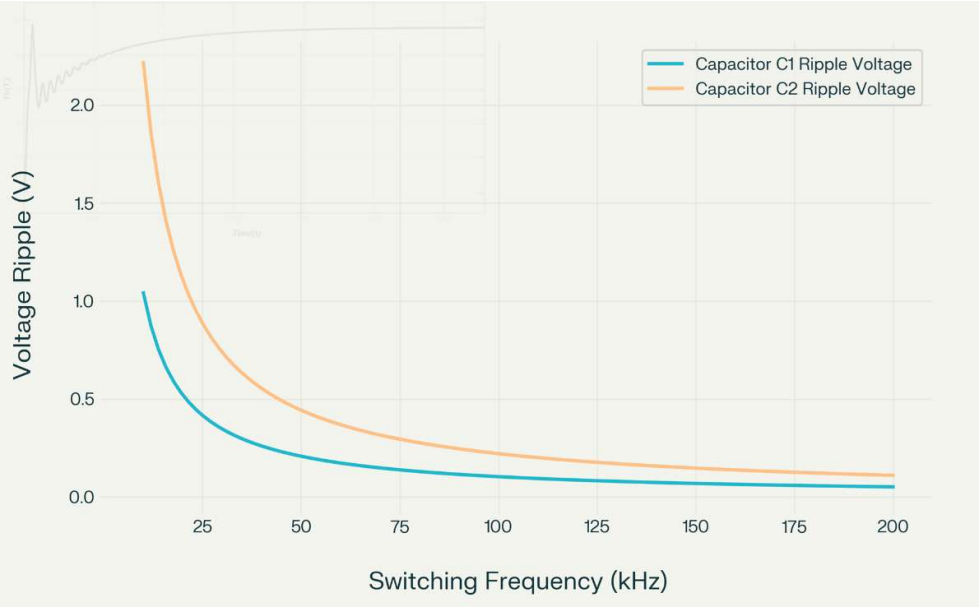

This skill to maintain a precise output voltage, which is especially remarkable in an open-loop system, highlights the efficiency of the converter as well as the correctness of its design and the selection of its components. There is a curious link between the output voltage and Switching Frequency, which is depicted in Figure 2.9. The switching frequency as well as the ripple. A clear and constant trend can be observed: as the switching frequency increases, there is a discernible decrease in the ripple that is present within the output voltage. Due to the fact that it shows that increasing the switching frequency can improve the output quality, this inverse relationship is extremely important for applications that require a smooth DC output.

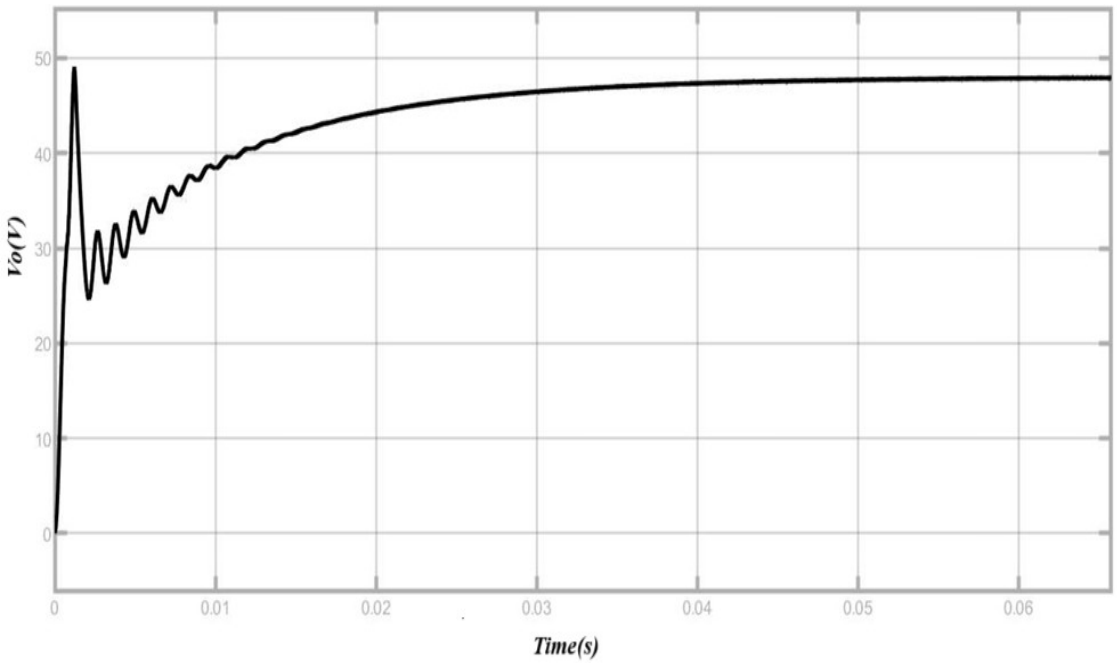

Fig 2.10: Output Voltage response at rated condition.

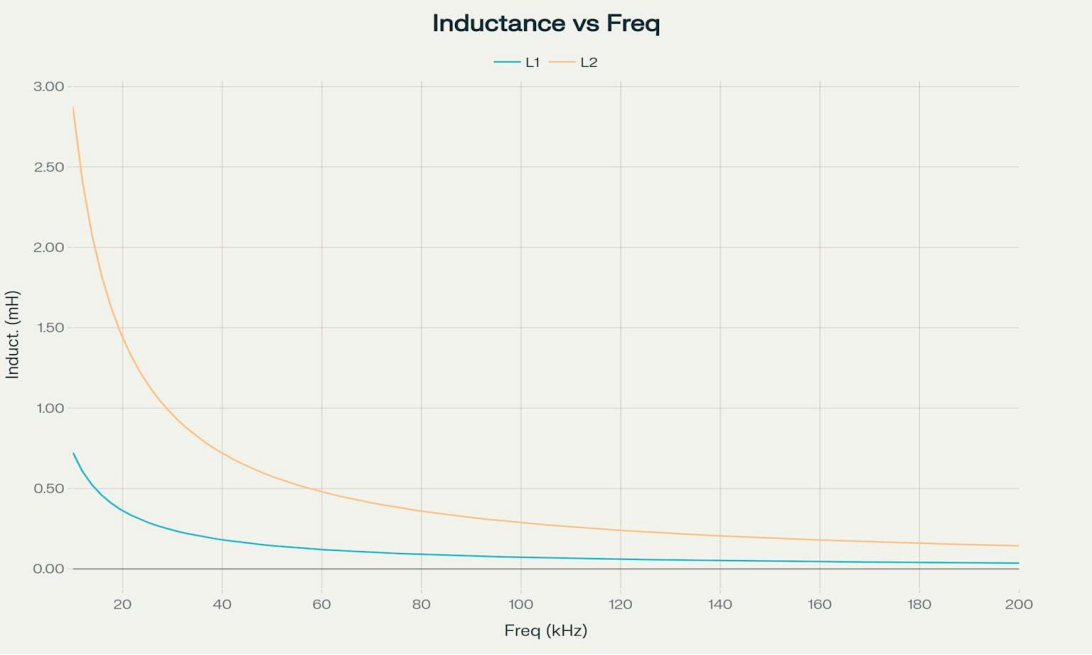

Fig 2.11: Relation of Frequency with Inductance L1 and L2.

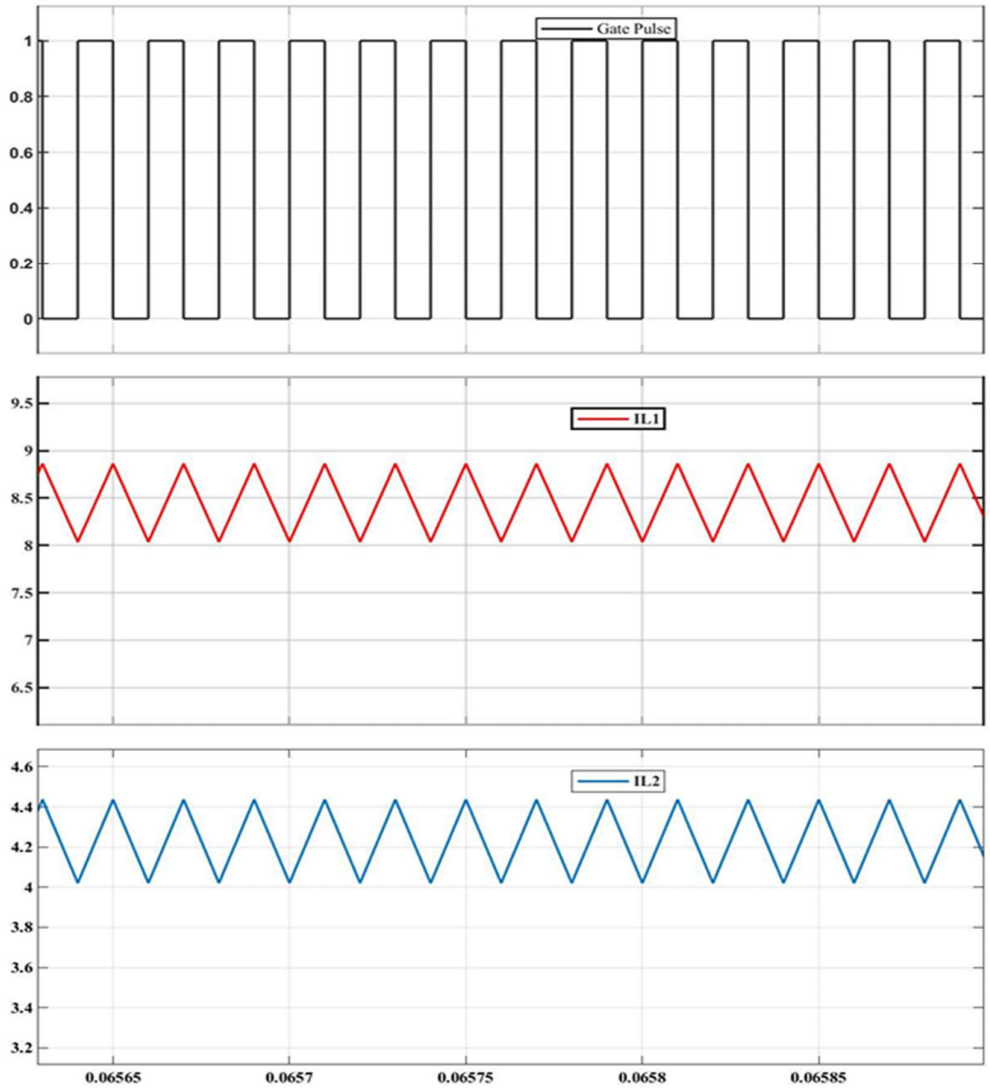

Fig 2.12: Current Profile of Inductor L1 and L2.

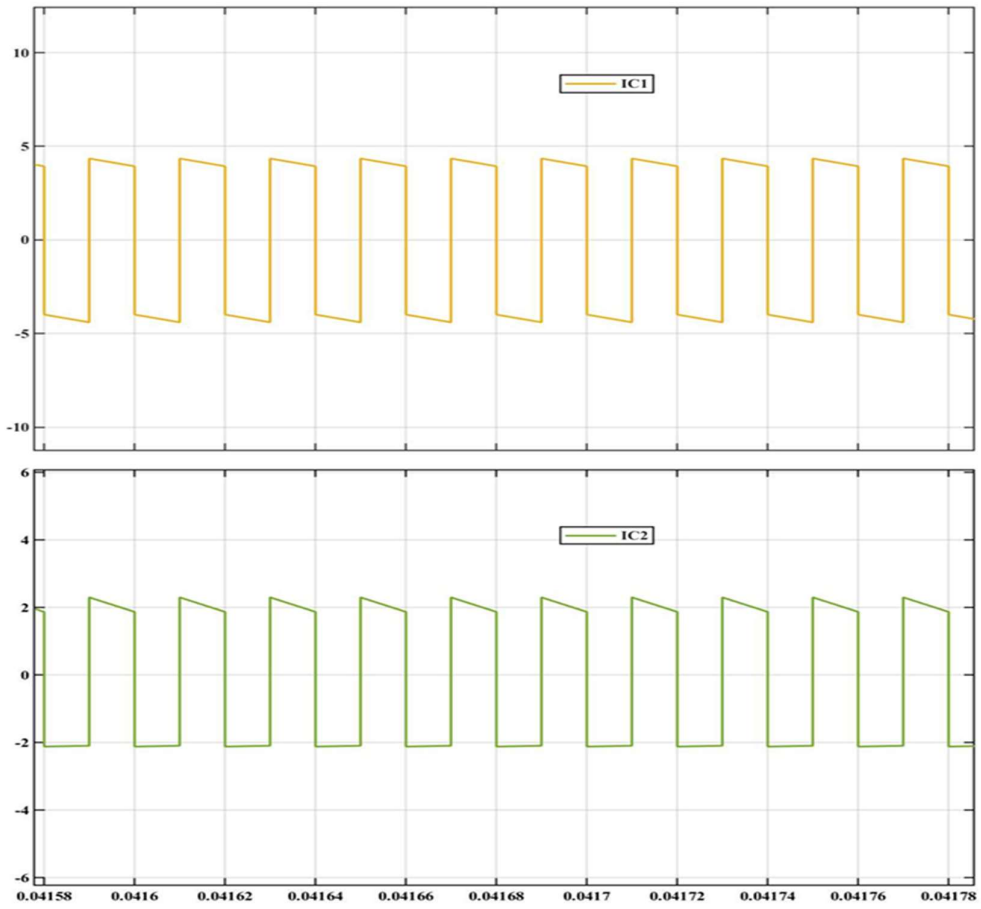

Fig 2.13: Current Profile of Capacitor C1 and C1.

Simultaneously, Figure 2.11 shows yet another fascinating link between the inductance value and the switching frequency. The data acquired reveals a drop in the required inductance value, which indicates that the switching frequency rises. The results of this study affect practically the design of Compact Quadratic Boost converters. Higher switching frequencies allow for the use of smaller inductors, which could lead to size and cost savings without sacrificing performance criteria.

CHAPTER 3

MODELLING OF DC-DC CONVERTERS

3.1 Introduction

Modeling DC-DC converters is a crucial first step in developing efficient power conversion systems. This process is crucial because it allows engineers and designers to predict how converters will react in different operating scenarios. By understanding how these converters respond to different loads, input voltages, and other environmental conditions, it is possible to optimize their performance, increase their efficiency, and ensure their reliability in practical applications.

In addition, modeling is important in the controller design for these converters. An accurate model makes it easier to develop a controller that can precisely manage the output voltage or current, maintain stability in dynamic circumstances, and respond to disturbances efficiently. This is especially significant in applications requiring high power efficiency and response speed, such as automotive, portable electronics, and renewable energy systems. The state-space averaging technique is extensively used in the thesis to explain the converters since it provides a simple yet accurate description of the system dynamics. This method bridges the gap between complex electrical systems and the practical requirement for smaller models that are simple to use and evaluate for control design.

3.2 State Space averaging Modelling Technique

The state-space averaging technique models and analyzes the dynamic behavior of power converters. This method transforms the nonlinear, switching nature of DC-DC converters into linear time-invariant (LTI) systems throughout a transitioning time. This allows for the use of linear control theory to develop and analyze converter controllers, making it easier and faster than dealing with nonlinear systems.

The method is made up of many steps. The first thing it does is figure out the converter's states (like "on" and "off") and model their circuit equations in state-space form. The duty cycle of the converter is used to average the state-space equations for one switching time. This makes a set of average state-space equations that describe

how the translator behaves over time. The state-space average method gives a complete picture of how well the converter works by putting together the electrical and control system features into a single framework. This all-around method is needed to improve converter design, performance, and reliability, as well as to make them better.

Engineers can use state-space averaging to create models that accurately reflect real-world behavior of both ideal and non-ideal DC-DC converters. This allows for efficient and resilient power conversion systems and controllers. The state-space averaging technique simplifies the analysis and design of power electronic converters by reducing their nonlinear behavior to linear time-invariant (LTI) models. The steps below demonstrate the generalized state space averaging modeling technique.

Step 1: Identify System States

The initial stage is to determine the several operational states of the converter. For a conventional switched-mode power supply, these states relate to the switching components (such as MOSFETs or diodes) being in either an 'on' or 'off' condition. Every operating condition of the DC-DC converter is characterized by its own set of system equations. Usually, the state variables chosen for modelling are the currents running through inductors and the voltages across capacitors. The total number of state variables therefore directly depends on the quantity of inductors and capacitors in the circuit. A state variable vector, represented as x(t), encapsulates these state variables. The state equations for the two operational circuit states under Continuous Conduction Mode (CCM) can be stated as follows:

I. When the MOSFET is on during the switching interval $0 < t < DT$, the state equation is given as:

$$\frac{dx(t)}{dt} = A_1 x(t) + B_1 u(t) \qquad 3.1$$

$$y(t) = E_1 x(t) + F_1 u(t) \qquad 3.2$$

II. When the MOSFET is off during the switching interval DT < t < T, the state equation is given as:

$$\frac{dx(t)}{dt} = A_2x(t) + B_2u(t) \quad 3.3$$

$$y(t) = E_2x(t) + F_2u(t) \quad 3.4$$

x(t) represents the state variable vector, encompassing inductor currents and capacitor voltages, with the controllable input indicated as u(t) and the output vector as y(t). The state matrix is represented as A, the input matrix as B, the output matrix as E, and the output coupling matrix as F.

Step 2: State Space Averaging equation:

Averaging the state equations across one switching period for every state variable, considering the duty cycle. Averaging over one switching interval removes the switching ripple component from the circuit equations. This means multiplying the state equations for the 'on' state by (D) and the equations for the 'off' state by (1-D), then adding these results together. By effectively linearizing the model in this way, one may analyze and design it using linear control theory.

$$\frac{d\bar{x}(t)}{dt} = A\bar{x}(t) + B\bar{u}(t) \quad 3.5$$

$$\bar{y}(t) = C\bar{x}(t) + D\bar{u}(t) \quad 3.6$$

Where,

$$A = A_1 * d(t) + A_2 * \big(1 - d(t)\big) \quad 3.7$$

$$B = B_1 * d(t) + B_2 * \big(1 - d(t)\big) \quad 3.8$$

$$E = E_1 * d(t) + E_2\big(1 - d(t)\big) \quad 3.9$$

$$F = F_1 * d(t) + F_2\big(1 - d(t)\big) \quad 3.10$$

In the framework of the averaged state-space model, the overline symbol (-) signifies the mean value of a variable across the complete duration of a switching period. The equations denoted as (3.5) and (3.6) demonstrate nonlinearity, resulting from the multiplication of time-dependent variables.

Step 3: Perturbation and Linearisation of averaged state space model

We use perturbation and linearization methods a lot to study and handle systems that don't behave in a straight line, like the averaged state-space models show. These use small changes around a steady operating point to get a rough idea of how the system will behave. This method makes it easier to come up with control strategies and analyze systems, especially in the field of power electronics.

The small ac perturbation introduced around steady state values are as follows:

$$\bar{x}(t) = X + \hat{x}(t) \ , \bar{y}(t) = Y + \hat{y}(t)$$
$$d(t) = D + \hat{d}(t), \quad d'(t) = 1 - d(t) = 1 - D - \hat{d}(t) = D' - \hat{d}(t) \tag{3.11}$$

It is to note that $X \gg \hat{x}(t), Y \gg \hat{y}(t), U \gg \hat{u}(t) and\ D \gg \hat{d}(t)$.

By substituting the eq. (3.11) into eq. (3.5) -(3.6) we get,

$$\dot{X} + \dot{\hat{x}}(t) = \left[A_1\left(D + \hat{d}(t)\right) + A_2\left(1 - D - \hat{d}(t)\right)\right]\left(X + \hat{x}(t)\right) + \left[B_1\left(D + \hat{d}(t)\right) + B_2\left(1 - D - \hat{d}(t)\right)\right]\left(U + \hat{u}(t)\right) \tag{3.12}$$

On simplifying we get,

$$\dot{X} + \dot{\hat{x}}(t) = \left[A_1 D + A_2(1 - D) + (A_1 - A_2)\hat{d}(t)\right]\left(X + \hat{x}(t)\right) + \left[B_1 D + B_2(1 - D) + (B_1 - B_2)\hat{d}\right]\left(U + \hat{u}(t)\right) \tag{3.13}$$

Similarly,

$$Y + \hat{y}(t) = \left[E_1\left(D + \hat{d}(t)\right) + E_2\left(1 - D - \hat{d}(t)\right)\right]\left(X + \hat{x}(t)\right) + \left[F_1\left(D + \hat{d}(t)\right) + F_2\left(1 - D - \hat{d}(t)\right)\right]\left(U + \hat{u}(t)\right) \tag{3.14}$$

Simplifying the above equation yields,

$$Y + \hat{y}(t) = \left[E_1 D + E_2(1 - D) + (E_1 - E_2)\hat{d}(t)\right]\left(X + \hat{x}(t)\right) + \left[F_1 D + F_2(1 - D) + (F_1 - F_2)\hat{d}\right]\left(U + \hat{u}(t)\right) \tag{3.15}$$

To formulate the linear model, we exclude the second-order nonlinear factors that result from the multiplication of two minor AC perturbed signals, as indicated in equations (3.13) to (3.15). Consequently, we derive:

$$\dot{X} + \dot{\hat{x}}(t) = \left(A_1 D + A_2(1 - D)\right)X + \left(A_1 D + A_2(1 - D)\right)\hat{x}(t) + (A_1 - A_2)X\hat{d}(t) + \left(B_1 D + B_2(1 - D)\right)U + \left(B_1 D + B_2(1 - D)\right)\hat{u}(t) + (B_1 - B_2)U\hat{d}(t) \tag{3.16}$$

$$Y + \hat{y}(t) = \big(E_1 D + E_2(1-D)\big)X + \big(E_1 D + E_2(1-D)\big)\hat{x}(t) + (E_1 - E_2)X\hat{d}(t) + \big(F_1 D + F_2(1-D)\big)U + \big(F_1 D + F_2(1-D)\big)\hat{u}(t) + (F_1 - F_2)U\hat{d}(t) \quad 3.17$$

Now the above equations can be written as:

$$\dot{X} + \dot{\hat{x}}(t) = AX + BU + A\hat{x}(t) + B\hat{u}(t) + [(A_1 - A_2)X + (B_1 - B_2)U]\hat{d}(t) \quad 3.18$$

$$Y + \hat{y}(t) = EX + FU + E\hat{x}(t) + F\hat{u}(t) + [(E_1 - E_2)X + (F_1 - F_2)U]\hat{d}(t) \quad 3.19$$

$$Where\ , A = A_1 D + A_2(1-D), B = B_1 D + B_2(1-D), E = E_1 D + E_2(1-D), F = F_1 D + F_2(1-D) \quad 3.20$$

3.3 Small Signal AC Model

Separating out the small signal ac terms from eq. (3.18) -(3.19), we get

$$\dot{\hat{x}} = A\hat{x}(t) + B\hat{u}(t) + [(A_1 - A_2)X + (B_1 - B_2)U]\hat{d}(t) \quad 3.21$$

$$\hat{y}(t) = E\hat{x}(t) + F\hat{u}(t) + [(E_1 - E_2)X + (F_1 - F_2)U]\hat{d}(t) \quad 3.22$$

To ascertain the various transfer functions, we employ the Laplace transform on the previously given state-space model, resulting in the following expression:

$$s\hat{x}(s) = A\hat{x}(s) + B\hat{u}(s) + [(A_1 - A_2)X(s) + (B_1 - B_2)U(s)]\hat{d}(s) \quad 3.23$$

$$\hat{y}(s) = E\hat{x}(s) + F\hat{u}(s) + [(E_1 - E_2)X(s) + (F_1 - F_2)U(s)]\hat{d}(s) \quad 3.24$$

Equations (3.23) and (3.24) provide the foundation for deriving various transfer functions pertinent to DC-DC converters. In the context of a DC-DC converter, the variable (x) pertains to the oscillations in inductor current and capacitor voltage, whereas (u) relates to changes in input voltage and load current. The symbol (d) denotes variations in the duty cycle, while (y) represents modifications in the output voltage. Through the analysis of these equations, we may get the transfer functions that delineate the link between these perturbations as specified in Equations (3.25) - (3.26).

The transfer functions connecting the duty cycle (d) and input variables (u) to the state variables (x) are articulated as follows:

$$\frac{\hat{x}(s)}{\hat{d}(s)} = (sI - A)^{-1}[(A_1 - A_2)X(s) + (B_1 - B_2)U(s)] \quad 3.25$$

$$\frac{\hat{x}(s)}{\hat{u}(s)} = (sI - A)^{-1}B \quad 3.26$$

The relationships between the duty cycle (d) and the input parameters (u) to the output response (y) are characterized by a set of transfer functions.

$$\frac{\hat{y}(s)}{\hat{d}(s)} = E(sI - A)^{-1}[(A_1 - A_2)X(s) + (B_1 - B_2)U(s)] + [(E_1 - E_2)X + (F_1 - F_2)U] \quad 3.27$$

$$\frac{\hat{y}(s)}{\hat{u}(s)} = E(sI - A)^{-1}B + F \quad 3.28$$

In the following subsections, we will derive the transfer functions for Quadratic Boost converter.

3.4 Modelling of Quadratic Boost Converter.

Modeling the Quadratic Boost converter necessitates comprehension of this fundamental circuit design, which aligns with the discourse in the preceding chapter. The circuit is defined by transient currents and voltages that fluctuate over time. Significantly, at the output step, an extra current source, referred to as (z(t)), is included. This change seeks to evaluate the dynamic impact of fluctuations in load current on the output voltage response.

This section concentrates on the modeling of a DC-DC quadratic boost converter. This analysis presumes the converter functions in Continuous Conduction Mode (CCM). During CCM operation, a DC-DC Quadratic Boost converter transitions between two distinct states: (a) when the MOSFET switch is active (conducting) and the diode is inactive (not conducting), and (b) when the MOSFET switch is inactive (not conducting) and the diode takes over (conducting). We derive the state-space equations for these two circuit states to enhance our comprehension of the converter's behavior.

Step 1: Identifying System States and obtain the state space equations.

i. Switch ON duration (0 < t < DT)

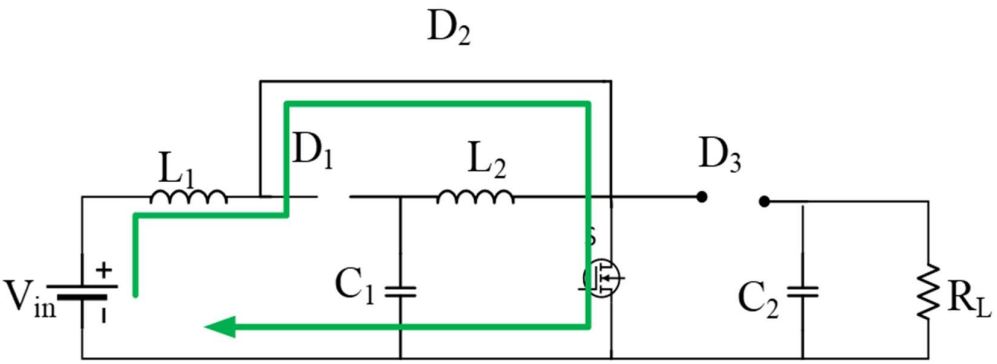

Fig 3.1: Circuit Diagram when Switch ON (MODE I).

The starting condition entails the switch, often a MOSFET, being in a closed position. This action facilitates energy transfer from the input source, through the inductors, and into the capacitors. According to Kirchhoff's voltage and current laws, the equations for inductor voltage, capacitor current, and output voltage are expressed as follows:

$$V_{L_1}(t) = L_1 \frac{di_{L_1}(t)}{dt} = V_s(t) \quad 3.29$$

$$V_{L_2}(t) = L_2 \frac{di_{L_2}(t)}{dt} = V_{C1}(t) \quad 3.30$$

$$i_{C_1}(t) = C_1 \frac{dV_{C_1}(t)}{dt} = i_{L_2}(t) \quad 3.31$$

$$i_{C_2}(t) = C_2 \frac{dV_{C_2}(t)}{dt} = -\frac{V_{C2}(t)}{R_o} \quad 3.32$$

$$V_o = V_{C_2}(t) \quad 3.33$$

Equations eq.(3.29)-eq.(3.33) can be written in state space representation as:

$$\begin{bmatrix} \frac{di_{L_1}}{dt} \\ \frac{di_{L_2}}{dt} \\ \frac{dV_{C_1}}{dt} \\ \frac{dV_{C_2}}{dt} \end{bmatrix} = A_1 \begin{bmatrix} i_{L_1} \\ i_{L_2} \\ V_{C_1} \\ V_{C_2} \end{bmatrix} + B_1[V_s] \quad 3.24$$

$$[V_o] = E_1 \begin{bmatrix} i_{L_1} \\ i_{L_2} \\ V_{C_1} \\ V_{C_2} \end{bmatrix} + F_1[V_s] \qquad 3.35$$

Where,

$$A_1 = \begin{bmatrix} 0 & 0 & 0 & 0 \\ 0 & 0 & 1 & -\frac{1}{L_2} \\ 0 & -\frac{1}{C_1} & 0 & 0 \\ 0 & 1 & 0 & \frac{-1}{R_o C_2} \end{bmatrix}, B_1 = \begin{bmatrix} \frac{1}{L_1} \\ 0 \\ 0 \\ 0 \end{bmatrix} \qquad 3.36$$

$$E_1 = [0 \quad 0 \quad 0 \quad 1], F_1 = [0]$$

ii. Switch OFF duration (DT< t < T)

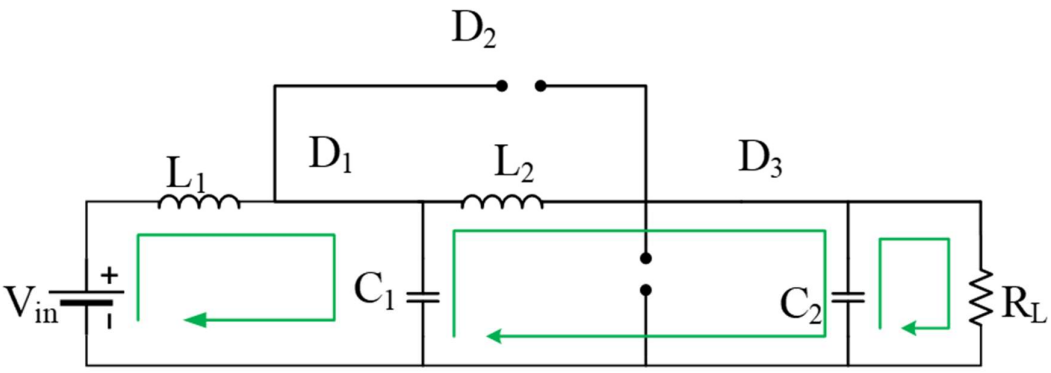

Fig 3.2: Circuit Diagram when Switch OFF (MODE II).

The diode conducts in the following state when the MOSFET switch is opened. A constant flow of energy from the capacitors to the output load is made possible by this transition. The following are the appropriate inductor voltages, capacitor currents, and output voltage equations obtained by applying Kirchhoff's voltage law and current law (KVL and KCL):

$$V_{L_1}(t) = L_1 \frac{di_{L_1}(t)}{dt} = V_s(t) - V_{C_1}(t) \quad 3.37$$

$$V_{L_2}(t) = L_2 \frac{di_{L_2}(t)}{dt} = V_{C_1}(t) - V_{C_2}(t) \quad 3.38$$

$$i_{C_1}(t) = C_1 \frac{dV_{C_1}(t)}{dt} = i_{L_1}(t) - i_{L_2}(t) \quad 3.39$$

$$i_{C_2}(t) = C_2 \frac{dV_{C_2}(t)}{dt} = i_{L_2}(t) - \frac{V_{C_2}(t)}{R_o} \quad 3.40$$

$$V_O(t) = V_{C_2}(t) \quad 3.41$$

Equations eq. (3.37)-eq. (3.41) can be written in state space representation as:

$$\begin{bmatrix} \frac{di_{L_1}}{dt} \\ \frac{di_{L_2}}{dt} \\ \frac{dV_{C_1}}{dt} \\ \frac{dV_{C_2}}{dt} \end{bmatrix} = A_2 \begin{bmatrix} i_{L_1} \\ i_{L_2} \\ V_{C_1} \\ V_{C_2} \end{bmatrix} + B_2[V_s] \quad 3.42$$

$$[V_o] = E_2 \begin{bmatrix} i_{L_1} \\ i_{L_2} \\ V_{C_1} \\ V_{C_2} \end{bmatrix} + F_2[V_s] \quad 3.43$$

Where,

$$A_2 = \begin{bmatrix} 0 & 0 & -\frac{1}{L_1} & 0 \\ 0 & 0 & 0 & -\frac{1}{L_2} \\ \frac{1}{C_1} & 0 & 0 & 0 \\ 0 & 1 & 0 & \frac{-1}{R_o C_2} \end{bmatrix}, B_2 = \begin{bmatrix} \frac{1}{L_1} \\ 0 \\ 0 \\ 0 \end{bmatrix} \quad 3.44$$

$$E_2 = [0 \quad 0 \quad 0 \quad 1], F_2 = [0]$$

Step 2: State Space Averaging Equations.

According to the discussed, the large-signal non-linear averaged state-space model of Quadratic Boost converter can be given as:

$$\begin{bmatrix} \frac{d\bar{\imath}_{L_1}}{dt} \\ \frac{d\bar{\imath}_{L_2}}{dt} \\ \frac{d\bar{V}_{C_1}}{dt} \\ \frac{d\bar{V}_{C_2}}{dt} \end{bmatrix} = \bar{A} \begin{bmatrix} \bar{\imath}_{L_1} \\ \bar{\imath}_{L_2} \\ \bar{V}_{C_1} \\ \bar{V}_{C_2} \end{bmatrix} + \bar{B}[\bar{V}_s] \quad 3.45$$

$$[\bar{V}_o] = \bar{E} \begin{bmatrix} i_{L_1} \\ i_{L_2} \\ V_{C_1} \\ V_{C_2} \end{bmatrix} + \bar{F}[\bar{V}_s] \quad 3.46$$

Where

$$\bar{A} = A_1 * D + A_2 * (1 - D), \bar{B} = B_1 * D + B_2 * (1 - D)$$
$$\bar{E} = E_1 * D + E_2 * (1 - D), \bar{F} = F_1 * d + F_2 * (1 - D) \quad 3.47$$

Step 3: Perturbation and Linearization of averaged state space model.

In this context, we add minor deviations to specific variables in relation to their standard, constant (DC) values. These modifications are implemented to analyze the system's behavior in proximity to its equilibrium or steady-state condition.

$$\bar{\imath}_{L_1}(t) = I_{L_1} + \hat{\imath}_{L_1}(t), \bar{\imath}_{L_2}(t) = I_{L_2} + \hat{\imath}_{L_2}(t)$$
$$\bar{V}_s(t) = V_s + \hat{v}_s(t), d(t) = D + \hat{d}(t) \quad 3.48$$
$$\bar{V}_{C_1}(t) = V_{C_1} + \hat{v}_{C_1}(t), \bar{V}_{C_2}(t) = V_{C_2} + \hat{v}_{C_2}(t), \bar{V}_o(t) = V_o + \hat{v}_o(t)$$

By introducing this perturbation, and ignoring the higher order ac terms we can obtain the small signal ac model of Quadratic Boost converter which will be given as:

$$\begin{bmatrix} \frac{d\hat{\imath}_{L_1}}{dt} \\ \frac{d\hat{\imath}_{L_2}}{dt} \\ \frac{d\hat{V}_{C_1}}{dt} \\ \frac{d\hat{V}_{C_2}}{dt} \end{bmatrix} = A \begin{bmatrix} \hat{\imath}_{L_1} \\ \hat{\imath}_{L_2} \\ \hat{V}_{C_1} \\ \hat{V}_{C_2} \end{bmatrix} + B[\hat{V}_s] \quad 3.49$$

$$[\hat{V}_o] = E \begin{bmatrix} \hat{\imath}_{L_1} \\ \hat{\imath}_{L_2} \\ \hat{V}_{C_1} \\ \hat{V}_{C_2} \end{bmatrix} + F[\hat{V}_s] \quad 3.50$$

Step 4: Derivation of Transfer Function:

Now, by taking the Laplace transform and using eq. (3.25) and eq. (3.28), We can calculate various transfer function.

I. **Line to Output voltage transfer function:**

The transfer function of input voltage to output voltage in a Quadratic Boost converter delineates the output voltage's reaction to fluctuations in the input voltage.

$$\frac{\hat{v}_o(s)}{\hat{v}_s(s)} = G_{vg}(s) = C(sI - A)^{-1}[B]_{first\ coloumn} \quad 3.51$$

$$G_{vg}(s) = \frac{\frac{DD'}{L_1L_2C_1C_2}}{s^4 + \frac{1}{RC_2}s^3 + \left(\frac{D'^2}{L_1C_1} + \frac{D^2}{L_2C_1} + \frac{1}{L_2C_2}\right)s^2 + \frac{D^2L_1 + D'^2L_2}{RL_1L_2C_1C_2}s + \frac{D'^2}{L_1L_2C_1C_2}} \quad 3.52$$

II. **Load Current to output voltage transfer Function:**

The Quadratic Boost converter's load current to output voltage transfer function shows how the voltage sent to the load changes as the load's current level changes. This shows that the converter can regulate the output voltage. This function is important for testing how the converter works with different loads to make sure it can keep the output voltage stable even when the load

current changes. Understanding this link helps improve the design of the converter so that it works better and is more reliable in real-world situations.

$$\frac{\hat{v}_o(s)}{\hat{\imath}_z(s)} = G_{vz}(s) = C(sI - A)^{-1}[B]_{second\ coloumn} \tag{3.53}$$

$$G_{vz}(s) = \frac{-\frac{1}{L_1L_2C_1C_3}(L_1L_2C_2s^3+(D^2L_1+D'^2L_2)s)}{s^4+\frac{1}{RC_2}s^3+\left(\frac{D'^2}{L_1C_1}+\frac{D^2}{L_2C_1}+\frac{1}{L_2C_2}\right)s^2+\frac{D^2L_1+D'^2L_2}{RL_1L_2C_1C_2}s+\frac{D'^2}{L_1L_2C_1C_2}} \tag{3.54}$$

III. Control to Output Transfer Function:

A Quadratic Boost converter has a function called duty cycle to output voltage transfer function that shows how changes in the duty cycle affect the output voltage. This relationship is very important for controlling and adjusting the voltage output to meet the load's specific needs. This makes sure that power is delivered efficiently in a wide range of working conditions.

$$\frac{\hat{v}_o(s)}{\hat{d}(s)} = G_{vd}(s) = C(sI - A)^{-1}[(A_1 - A_2)X + (B_1 - B_2)U] \tag{3.55}$$

$$G_{vd}(s) = \frac{-\frac{1}{L_1L_2C_1C_2}\left(L_1C_1V_{C_1}s^2 - L_1I_{L_1}s + D'V_{C_1}\right)}{s^4 + \frac{1}{RC_2}s^3 + \left(\frac{D'^2}{L_1C_1} + \frac{D^2}{L_2C_1} + \frac{1}{L_2C_2}\right)s^2 + \frac{D^2L_1 + D'^2L_2}{RL_1L_2C_1C_2}s + \frac{D'^2}{L_1L_2C_1C_2}} \tag{3.56}$$

CHAPTER 4

SLIDING MODE CONTROLOF QUADRATIC BOOST CONVERTERS

4.1 Introduction.

The growth of Sliding Mode Control (SMC) indicates that control theory is shifting toward more flexible and better approaches. Very distinct from this approach are older control techniques, which have been widely discussed in this thesis and which largely depend on transfer functions. Though they don't naturally fit with nonlinear systems like DC-DC converters, these ancient methods of doing things are quite beneficial for comprehending linear systems. Things become more difficult as these systems are not linear. This makes it difficult for conventional control techniques to manage them properly, which results poor performance. One major issue with these antiquated techniques is their foundation on the notion that items are simple and unchanging across time. In the actual world, where things vary and don't follow a straight line, this is not always the case. These techniques are vulnerable to variations in parameters and outside interference; hence this discrepancy could result in less precise and dependable control. The previous techniques also don't always handle the high switching frequencies typical in modern power systems efficiently, which could affect performance and responsiveness not as well as they might be.

Sliding Mode Control is a very good choice in this case since it was meant to cope with the challenges of nonlinear systems. SMC is unique since its robust architecture ignores variations in system characteristics or external source delays. A particular control technique pushing the system states to fit onto a well-defined sliding surface makes this feasible. This guarantees that even with disturbances or changes in system parameters, the system operates at its optimum.

A slide mode control system is put together in a number of well-thought-out steps. To begin, it is important to explain what a sliding surface is. This is a key part that shows the system's ideal state progress. It was very careful when making this surface so that once the system's state hits it, it will stay in this dynamic regime and keep changing. It's important to make a reaching rule after this. No matter

how the system starts, this law tells you what management steps you need to take to get it to the sliding surface in a certain amount of time. The last step is to put the control law into effect. This means that we need to turn on the control inputs that will keep the system's state on the moving surface and make sure it acts the way we want it to. When you use Sliding Mode Control, you get a lot of important benefits. Its reliability and performance remain high in a wide range of working conditions are due to its ability to handle different types of disturbances and its insensitivity to changes in system parameters. For this reason, SMC works really well when other control methods don't work well with difficult, nonlinear systems. SMC is also very responsive and efficient because it can handle high switching rates. This makes it an even more popular choice for current engineering problems.

Finally, Sliding Mode Control comes out as a sophisticated way to control systems that does a good job of getting around the problems that regular methods based on transfer functions have, especially when working with systems that are not linear. A SMC robust and adaptive design theory is made up of three steps: defining a sliding surface, making a reaching law, and setting up a control law. This way of thinking gives SMC a big advantage when it comes to speed reliability and being able to handle changes and unknowns. Because of this, it is a big step forward in control theory, giving us better tools to work with the complicated systems we see in modern engineering.

4.2 Dynamic Equation of Quadratic Boost Converter.

I. **MODE 1:** When the Quadratic Boost converter is working in MODE 1, the switch S is closed and the input voltage is sent to the inductor L1. This lets the input current flow through inductor L1, which makes the current across L1 rise slowly but steadily. In this step, diode D1 and D3 stays biased in the opposite direction and D2 conduct, which lets the energy stored in coupling capacitor C1 be sent to output capacitor C2 and the load through inductor L2. So,

$$V_{L_1}(t) = L_1 \frac{di_{L_1}(t)}{dt} = V_s(t) \qquad 4.1$$

$$V_{L_2}(t) = L_2 \frac{di_{L_2}(t)}{dt} = V_{C1}(t) \quad 4.2$$

$$i_{C_1}(t) = C_1 \frac{dV_{C_1}(t)}{dt} = i_{L_2}(t) \quad 4.3$$

$$i_{C_2}(t) = C_2 \frac{dV_{C_2}(t)}{dt} = -\frac{V_{C2}(t)}{R_o} \quad 4.4$$

$$V_o = V_{C_2}(t) \quad 4.5$$

II. **MODE 2:** The switch S is open during MODE 2. This connects the inductor L1 to the coupling capacitor C1 in series. This setup makes it easy to move energy from the L1 storage to the C1 storage. At the same time, it moves energy from the L2 storage to both the output capacitor C2 and the load. During this time, we have:

$$V_{L_1}(t) = L_1 \frac{di_{L_1}(t)}{dt} = V_s(t) - V_{C_1}(t) \quad 4.6$$

$$V_{L_2}(t) = L_2 \frac{di_{L_2}(t)}{dt} = V_{C_1}(t) - V_{C_2}(t) \quad 4.7$$

$$i_{C_1}(t) = C_1 \frac{dV_{C_1}(t)}{dt} = i_{L_1}(t) - i_{L_2}(t) \quad 4.8$$

$$i_{C_2}(t) = C_2 \frac{dV_{C_2}(t)}{dt} = i_{L_2}(t) - \frac{V_{C_2}(t)}{R_o} \quad 4.9$$

$$V_O(t) = V_{C_2}(t) \quad 4.10$$

The equations governing the dynamics when the switch is turned on and off can be merged in the following manner:

$$\frac{di_{L_1}(t)}{dt} = \frac{1}{L_1}\left[V_s(t) - \bar{d}V_{C_1}(t)\right] \quad 4.11$$

$$\frac{di_{L_2}(t)}{dt} = \frac{1}{L_2}\left[dV_{C_1}(t) - V_{C2}(t)\right] \quad 4.12$$

$$\frac{dV_{C_1}(t)}{dt} = \frac{1}{C_1}\left[\bar{d}i_{L_1}(t) - di_{L_2}(t)\right] \quad 4.11$$

$$\frac{dV_{C_2}(t)}{dt} = \frac{1}{C_2}\left[i_{L_2}(t) - \frac{V_{C2}(t)}{R_o}\right] \quad 4.12$$

Where $\bar{u}$=1-u and represents a binary switching signal that takes the value of 1 when the switch is on, and 0 when it is off.

4.3 Designing of Sliding Mode Control for Quadratic Boost Converter.

The design of a sliding mode control for a Quadratic Boost converter is a methodical approach to governing the performance of the converter by utilizing two control loops that are distinct from one another yet are linked together. This idea is quite ingenious, which includes both an outer voltage control loop and an inner current control loop simultaneously. A Proportional-Integral (PI) controller is utilized in the outer loop in order to exercise control over the voltage. Through the implementation of adjustments that aim to decrease both steady-state and transient defects, this ensures that the output will always correspond to the setpoint that has been specified. On the other hand, the inner loop makes use of a sliding mode controller, which is a powerful approach that is well-known for its capacity to reject disturbances and remain stable even when the parameters of the system are altered.

It has been decided that the main inductor current (i_{L1}) and the output voltage (V_o) will be the state variables that will be regulated for the sliding mode control of the Quadratic Boost converter. Each and every time, the control system is provided with the values of these variables in real time. Through the use of this feedback system, the system is able to adapt while maintaining the output voltage within predetermined parameters. Through the process of monitoring and reacting to changes in iL1 and vo, the sliding mode controller that is located in the inner current loop is able to quickly resolve any issues that may arise. This ensures that the converter remains steady and improves the reliability of the power quality.

Table 4.1: Controller Design Parameter for Quadratic Boost converter.

Parameters	Values
Input Voltage Vs	12V
Output Voltage Vo	48V
Load Resistance Ro	23.0.4Ω
Inductance L1	$145\mu H$
Inductance L2	$576\mu H$
Capacitor C1	$200\mu F$
Filter Capacitor C2	$47\mu F$
Switching Frequency fs	50KHz
Desired Inductor Current Ripple$\Delta i_{L1}/\Delta i_{L2}$	$10\%I_{L1}/10\%I_{L2}$
Desired Output Voltage Ripple Current Ripple$\Delta V_{C1}/\Delta V_{C2}$	$1\%V_{C1}/1\%V_{C2}$

I. **Outer voltage loop controller:** The outer voltage loop in a Quadratic Boost Converter control system is primarily responsible for mitigating and, preferably, eliminating the steady-state error in the output voltage. This is the major role of the outer voltage loop. It is necessary to strategically insert a proportional-integral (PI) controller into the loop in order to reach this degree of precision and stability. Because it combines the instant responsiveness of proportional control to output voltage deviations with the ability of integral action to minimize residual steady-state mistakes over time, a PI controller is extremely well-suited for this purpose. This is because the workings of a PI controller combine these two characteristics. This particular PI controller does not immediately alter the settings of the converter when it is generated as an output. However, it serves as a reference goal for the principal inductor current(i_{ref}).

$$i_{ref} = K_{prop}e(t) + \int K_C\, e(t)dt \qquad 4.15$$

$$e(t) = V_{ref} - \beta V_o \qquad 4.16$$

This reference serves as a bridge between the desired output voltage stabilization objectives and the dynamic operational adjustments executed by

the inner current control loop.

II. **Inner current loop controller:** The inner current loop has a very different job than the outer voltage loop. Its job is to control the real inductor current ($iL1$) so that it matches a specified reference current ($iref$) that the outside loop has established. This is where picking a sliding mode controller becomes very important. The controller changes the states of the semiconductor switches in the converter on the fly by constantly comparing the actual and reference inductor currents. It uses a carefully designed sliding surface to figure out the best times to flip these switches, making sure that the real inductor current always matches its reference. This approach not only helps the outer loop stabilize the voltage, but it also makes the Quadratic Boost converter more efficient and reliable by keeping exact current management even when the load changes.

4.4 Defining of Control Equivalent Model.

Sliding mode control operates by modifying the system's dynamics to compel the system's state onto a specified sliding surface, subsequently ensuring its maintenance on this surface despite disturbances or uncertainties inside the system. The sliding surface is essential since it delineates the intended system behavior in the control process. Selecting a suitable sliding surface is crucial for guaranteeing the strong performance and stability of the control system, enabling it to respond predictably to changes and disturbances. To attain this control, sliding mode control alternates among many control rules, striving for accuracy and dependability in achieving the system's intended state. The creation of an ideal sliding surface is crucial, since it determines the trajectory to the desired state and substantially affects the system's response time and efficiency. This meticulous selection guarantees that the system maneuvers through disturbances with minimal departure from its trajectory, highlighting the necessity of customizing the sliding surface to the system's particular requirements and attributes. Obtaining a control-oriented model is essential for

deriving a simpler equivalent control rule. This model illustrates the error dynamics of the DC-DC Quadratic Boost converter operating in Continuous Conduction Mode (CCM).

Sliding-mode current control involves the selection of a certain reference current signal, i_{ref} to guide the operation of the system as follows:

$$i_{ref} = K_c\,(V_{ref} - \beta V_o) \tag{4.17}$$

For developing the control-centric model of the DC-DC Cuk converter, selecting the appropriate control state variables is crucial. In this context, the control state variable is identified as:

$$x_1 = i_{ref} - i_{L_1} \tag{4.18}$$

$$x_2 = \int \left(V_{ref} - \beta V_o\right) dt \tag{4.19}$$

$$x_3 = \int x_1 dt \tag{4.20}$$

$$x_4 = \int x_2 dt \tag{4.21}$$

The system under consideration includes four state variables, namely (x_1, x_2, x_3), and (x_4), which serve distinctive purposes in representing the system's dynamics. The variable (x_1) is responsible for capturing the discrepancy in the input inductor current from its desired value. Meanwhile, (x_2) is the cumulative sum, or integral, of the difference in the output voltage from its intended target, offering a sense of how this error evolves over time.

Delving further, (x_3) represents the integral of (x_1), which could be seen as a secondary measure of the current error's long-term behavior. (x_1) extends this concept by being the integral of (x_2), effectively becoming the double-integral of the output voltage error. The significance of (x_4) lies in its role in the control system—it is instrumental in addressing and mitigating any persistent discrepancy in the output voltage, thereby working to secure a steady state output with minimal error.

These variables encapsulate the converter's control dynamics, offering a precise representation that's essential for effective management and control of the system's behavior as shown below:

$$\dot{x_1} = -K_c\beta \frac{dV_o}{dt} - \frac{di_{L_1}}{dt} \tag{4.22}$$

$$\dot{x_2} = V_{ref} - \beta V_o \tag{4.23}$$

$$\dot{x_3} = i_{ref} - i_{L_1} \tag{4.24}$$

$$\dot{x_4} = \int V_{ref} - \beta V_o \quad 4.25$$

In alignment with averaging theory, the control-oriented model of the DC-DC Cuk converter, as derived from eq. (5.11) -(5.14), is delineated by the following equation:

$$\dot{x_1} = -\frac{K_c \beta i_{C_2}}{C_2} - \frac{\left(V_s - V_{C_1} \underline{D}\right)}{L_1} \quad 4.26$$

$$\dot{x_2} = V_{ref} - \beta V_o \quad 4.27$$

$$\dot{x_3} = i_{ref} - i_{L_1} \quad 4.28$$

$$\dot{x_4} = \int V_{ref} - \beta V_o \quad 4.29$$

4.5 Derivation of equivalent control Law.

The implementation of sliding mode control (SMC) in quadratic boost converters requires a meticulously constructed switching control input to fulfill the necessary hitting condition. Initially, identifying a suitable sliding surface is a critical step in effective SMC implementation, as seen below:

$$\epsilon(x) = m_1 x_1 + m_2 x_2 + m_3 x_3 + m_4 x_4 \quad 4.30$$

Where m1, m2, m3 and m4 are sliding coefficients.

A control input utilizing switching mechanisms must meet a particular requirement termed the hitting condition. This condition is crucial for the efficacy of the control method, guaranteeing that the system's reaction conforms to established performance requirements. To satisfy this criterion, the control input is adjusted to provoke a switching action, directing the system towards the sliding surface as delineated by the equation:

$$d_{eq} = \frac{1}{2}(1 + sign(\epsilon)) \quad 4.31$$

According to the hitting condition in SMC, the derivative of the sliding surface ($\epsilon(x)$) along the system trajectories should be zero or negative definite, formally expressed as:

$$\dot{\epsilon}(x) = m_1 \dot{x_1} + m_2 \dot{x_2} + m_3 \dot{x_3} + m_4 \dot{x_4} \quad 4.32$$

According to the principles of invariance, the error dynamics of the dc-dc Quadratic

boost converter diminish to zero upon attaining the sliding surface. The subsequent stage involves the incorporation of the model, which is averaged and customized for control purposes, into eqn. (5.28). This integration provides enhanced understanding of the converter's performance under specified operational settings.

$$m_1\left(-\frac{K_c\beta}{C_2}i_{C_2}-\frac{V_s-V_{C_1}d_{eq}}{L_1}\right)+m_2\left(V_{ref}-\beta V_o\right)+m_3\left(i_{ref}-i_{L_1}\right)+ m_4\left[\int\left(V_{ref}-\beta V_o\right)dt\right]=0 \quad (4.33)$$

In steady-state operation, the average current through the capacitor is essentially zero. Furthermore, this aspect does not significantly affect the sliding-mode control methodology, particularly in comparison to the influence of other control state variables. Consequently,

$$m_1\left(-\frac{V_s-V_{C_1}d_{eq}}{L_1}\right)+m_2\left(V_{ref}-\beta V_o\right)+m_3\left(i_{ref}-i_{L_1}\right)+ m_4\left[\int\left(V_{ref}-\beta V_o\right)dt\right]=0 \quad (4.34)$$

In a Quadratic Boost converter, the switching control input (u) typically involves the alternation between two state scenarios—engaging and disengaging the switch, contingent on the status of ϵ(x). This leads to the expression of the control law as:

$$d_{eq}=\frac{1}{V_{C_1}}\left(\left(V_{C_1}-V_S\right)-K_cI_{L_1}+K_{prop}\left(V_{ref}-\beta V_o\right)+K_{int}\left(\int\left(V_{ref}-\beta V_o\right)dt\right)\right) \quad (4.35)$$

Where $\left[K_c, K_{prop}, K_{int}\right]=\left[\frac{m_3}{m_1}L_1,\ \frac{K_cm_3+m_2}{m_1}L_1,\ \frac{m_4}{m_1}L_1\right]$

4.6 Existence and stability conditions.

In sliding mode control (SMC), a fundamental need for obtaining optimal dynamic and steady-state performance is ensuring that the closed-loop system attains and maintains sliding mode (SM) functioning. A crucial prerequisite in this context is the hitting condition, which ensures that the system's state trajectory consistently converges towards the sliding surface, irrespective of the initial conditions. In the

case of the Quadratic Boost converter, the hitting condition is well fulfilled by suitably delineating the sliding surface.

4.7 Reference Voltage Tracking.

The reference voltage tracking performance of Quadratic Boost converters was assessed under dual-loop PI control and Sliding Mode Control (SMC) as depicted in Fig.4.1. The reference voltage was incrementally adjusted in increments, commencing at 24V and rising to 60V.

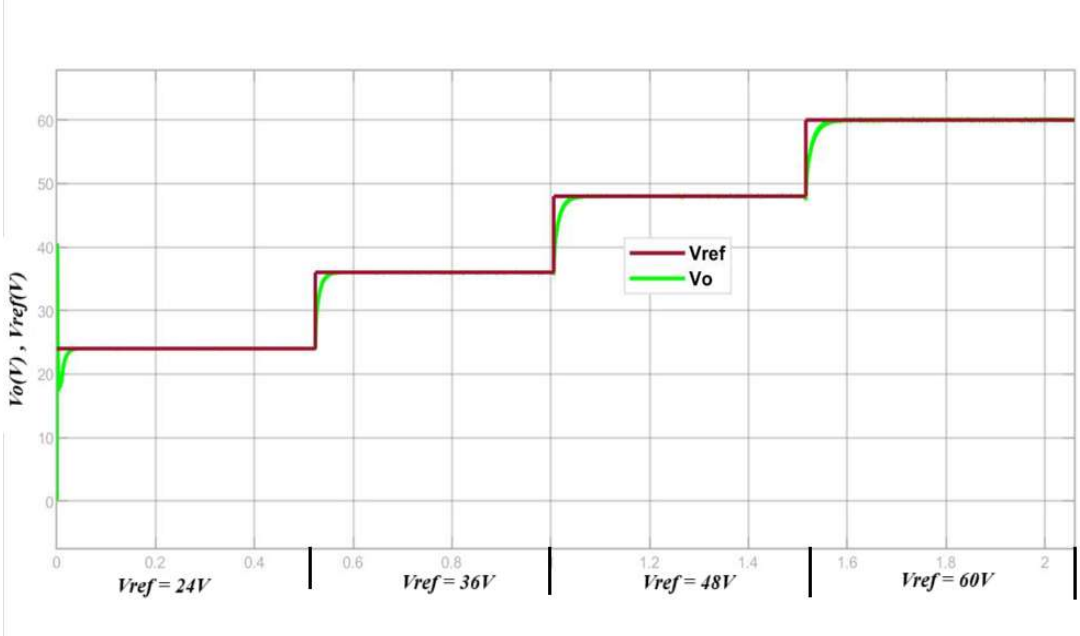

Fig 4.1: Reference Voltage Tracking for SMC.

4.8 Load Variation Transients.

The Fig.4.2 shows the load variation response in a Closed Loop Quadratic Boost Converter from 23 ohm to 5.75 ohm. Fig. 4.3 shows the line voltage response from 12V to 30V.

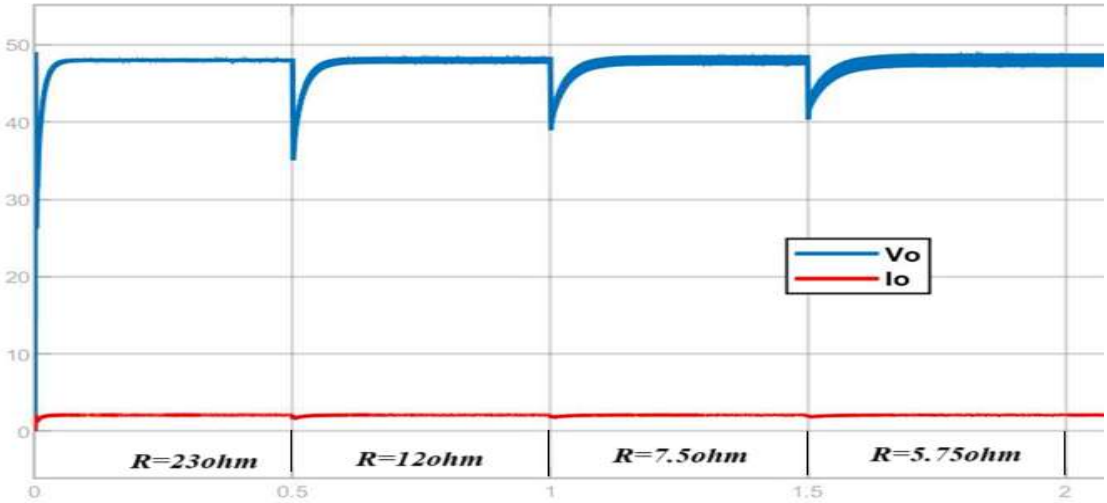

Fig 4.2: Response of Quadratic Boost converter under step variation of Load Resistance.

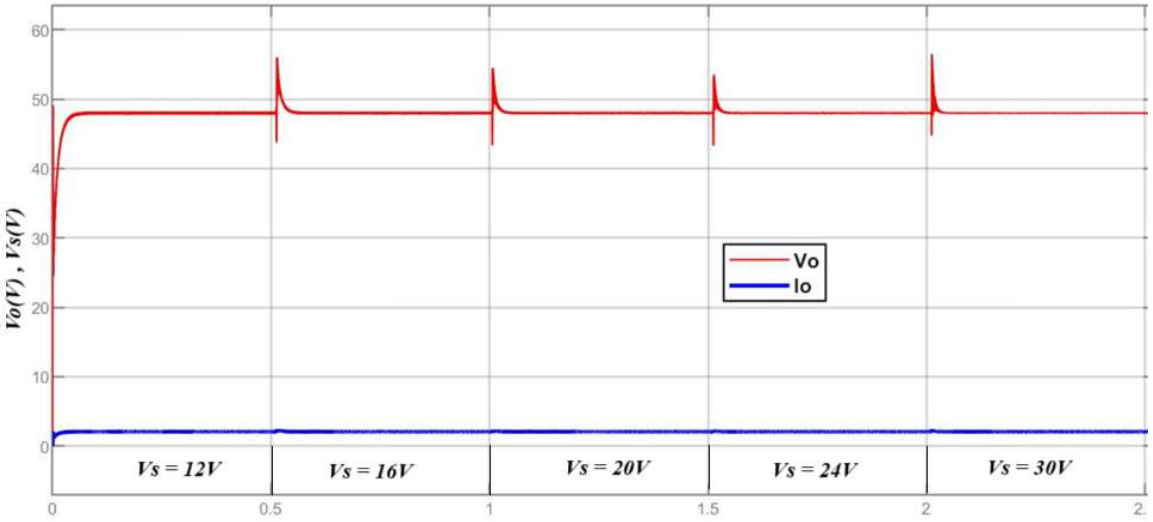

Fig 4.3: Response of Quadratic Boost converter under step variation of Line Voltage.

CHAPTER 5

CONCLUSION AND FUTURE SCOPE

5.1 Conclusion.

This thesis illustrated the effective application of sliding mode control (SMC) combined with proportional-integral (PI) correction for resilient voltage regulation in a quadratic boost converter (QBC). The hybrid control technique successfully sustained a consistent 48V output from a 12V input amidst dynamic load fluctuations (25–50% load variations), with less than 2% output voltage variance. The SMC facilitated rapid current adjustment of the input inductor, enhancing resilience to parameter uncertainties, while the outer PI loop reduced steady-state voltage inaccuracy. Experimental and modeling findings confirmed the controller's capability to reduce output ripple to less than 5% while sustaining 93% efficiency under full load conditions. The study emphasizes the QBC's appropriateness for renewable energy systems that necessitate high gain and stability. The state-space averaging method was utilized to examine the correlations among input voltage and output voltage, load current and output voltage, and duty cycle and output voltage for Quadratic Boost converters.

The last part of the thesis is all about how to use sliding mode control with the DC-DC Quadratic Boost converter. The development and analysis of the transfer functions gave us a new way of looking at things compared to earlier research. We used a direct way to calibrate the controller settings, and the Routh-Hurwitz stability criterion had an effect on this. The simulation tests showed that the sliding mode control worked just as well as the two-loop PI control system. Sliding mode control is better since it only needs to tune one PI controller, while the two-loop system needs to tune two. Additionally, this method does away with the need for a PWM modulator to create switching signals, making the entire control process easier.

5.2 Future Scope.

The research presented in this thesis paves the way for additional exploration and expansion:

I. The controller's capacity to separate voltage and current management mitigates issues in nano grids and irrigation-powered electric vehicle charging, where extensive input ranges and transient loads frequently occur. Future research may investigate adaptive SMC for broader operational ranges or fault-tolerant topologies to further augment reliability.

II. The approaches employed for the design, modeling, and control of DC-DC buck and Cuk converters can be readily adapted and modified for different varieties of DC-DC converters.

III. The small-signal average model employed in this thesis offers useful insights. Yet, it inadequately captures the comprehensive impact of converter switching frequency on system dynamics. Additional study could focus on creating mathematical models that explicitly account for the effects of converter switching frequency.

IV. The suggested control design approaches possess significant potential for application across various domains, including battery-operated electric cars, solar systems, and DC microgrids, among others. Continued investigation of these areas may yield significant insights and practical applications.

V. This thesis presents the development of control techniques with a focus on consistent converter parameters. Nevertheless, additional enhancements can be achieved in these systems by taking into account the fluctuations in converter parameters.

References

[1] N. Mohan, T. M. Undeland, and W. P. Robbins, Power Electronics-Converters, Applications and Design, 3rd ed. John Wiley, 2003.

[2]. M. H. Rashid, Power Electronics Handbook, 2nd ed. Academic Press, 2001.

[3]. R. W. Erickson and D. Maksimovic, Fundamentals of Power Electronics, 2nd ed. Kluwer Academic Publishers, 2001

[4]. P. T. Krein, Elements of Power Electronics. Oxford University Press, New York,1998.

[5]. B. K. Bose, "Need a Switch?," IEEE Ind. Electron. Mag., vol. 1, no. 4, pp. 30 39,Jan. 2007.

[6]. B. K. Bose, "Evaluation of modern power semiconductor devices and future trends of converters," IEEE Trans. Ind. Appl., vol. 28, no. 2, pp.403–413, 1992.

[7]. P. Imbertson and N. Mohan, "A method for estimating switch-mode power supply size," in Proceedings, Fourth Annual IEEE Applied Power Electronics Conference and Exposition, 1989, pp. 344–352

[8]. R. Silva-Ortigoza, V. M. Hernandez-Guzman, M. Antonio-Cruz, and D. Munoz Carrillo, "DC/DC Buck Power Converter as a Smooth Starter for a DC Motor Based on a Hierarchical Control," IEEE Trans. Power Electron., vol. 30, no. 2, pp. 1076–1084, 2015.

[9].]B. Singh and S. Singh, "Single-phase power factor controller topologies for permanent magnet brushless DC motor drives," IET Power Electron., vol. 3, no. 2, pp. 147–175, 2010.

[10]. B. Singh, S. Singh, and G. Bhuvaneswari, "Analysis and Design of a Zeta Converter Based Three-Phase Switched Mode Power Supply," in 4th International Conference on Computational Intelligence and Communication Networks, 2012, pp. 571–575

[11]. M. Dalla Costa, J. Alonso, T. Marchesan, M. Cervi, and R. Prado, "Electronic Ballasts for HID Lamps," IEEE Ind. Appl. Mag., vol. 17, no. 2, pp. 54–59, 2011.

[12]. J. Reginaldo de Britto, A. Elias Demian Junior, L. C. de Freitas, V. J. Farias, and E. A. A. Coelho, "Zeta DC/DC converter used as led lamp drive," in European Conference on Power Electronics and Applications, 2007, pp. 1–7. 136

[13]. H. Qiao, Y. Zhang, Y. Yao, and L. Wei, "Analysis of Buck-Boost Converters for Fuel Cell Electric Vehicles," in IEEE International Conference on Vehicular Electronics and Safety, 2006, pp. 109–113.

[14]. W.-Y. Choi, J.-M. Kwon, and B.-H. Kwon, "High-performance front-end rectifier system for telecommunication power supplies," vol. 153, no. 4. pp. 473–482, 2006.

[15]. A. Hussain, A. Kumar, and L. Behera, "Sliding mode control of a buck converter for maximum power point tracking of a solar panel," in 2013 IEEE International Conference on Control Applications (CCA), 2013, pp. 661–666.

[16]. N. Adhikari, B. Singh, A. L. Vyas, and A. Chandra, "Analysis and design of

isolated solar-PV energy generating system," in 2011 IEEE Industry Applications Society Annual Meeting, 2011, pp. 1–6.
[17]. M. G. Villalva, T. G. de Siqueira, and E. Ruppert, "Voltage regulation of photovoltaic arrays: small-signal analysis and control design," IET Power Electron., vol. 3, no. 6, p. 869, 2010.
[18]. S. Singh, G. Bhuvaneswari, and B. Singh, "Power quality improvement in telecommunication power supply system using buck rectifier," in IEEE India Conference, 2011, pp. 1–4.
[19]. N. Men dalek, K. Al-Haddad, A. Chandra, R. Parimelalagan, and V. Rajagopalan, "A new control strategy for DC voltage regulation and VAr generation using PWM three-phase rectifier," in Proceedings of Power and Energy Systems in Converging Markets, 1997, pp. 426–430.
[20]. K. M. Vijayalakshmi, M. G. Uma Maheswari, and G. Uma, "Analysis and design of reduced-order sliding-mode controller for three-phase power factor correction using Cuk rectifiers," IET Power Electron., vol. 6, no. 5, pp. 935–945, 2013.
[21]. C. H. Rivetta, A. Emadi, G. A. Williamson, R. Jayabalan, and B. Fahimi, "Analysis and control of a buck DC-DC converter operating with constant power load in sea and undersea vehicles," IEEE Trans. Ind. Appl., vol. 42, no. 2, pp. 559– 572, 2006.
[22]. R. Tymerski and V. Vorperian, "Generation and classification of PWM DC-toDC converters," IEEE Trans. Aerosp. Electron. Syst., vol. 24, no. 6, pp. 743–754, Nov. 1988.
[23]. B. Bryant and M. K. Kazimierezuk, "Derivation of the buck-boost PWM DC-DC converter circuit topology," in IEEE International Symposium on Circuits and Systems Proceedings, 2002, vol. 5, pp. V–841–V–844.
[24]. S. Cuk and R. D. Middlebrook, "A new optimum topology switching DC- toDC converter," in 1977 IEEE Power Electronics Specialists Conference, 1977, pp. 160–179.
[25]. S. Cuk, "Modelling, analysis, and design of switching converters," Ph.D thesis, California Institute of Technology, 1977.
[26]. D. C. Martins and G. N. de Abreu, "Application of the ZETA converter in switchedmode power supplies," in Conference Record of the Power Conversion Conference -Yokohama 1993, 1993, pp. 147–152.
[27]. M. K. Kazimierczuk and J.J. Jozwik, "Optimal topologies of resonant DC/DC converters," IEEE Trans. Aerosp. Electron. Syst., vol. 25, no. 3, pp. 363– 372, May 1989.
[28]. J. J. Jozwik and M. K. Kazimierczuk, "Dual sepic PWM switching-mode DC/DC power converter," IEEE Trans. Ind. Electron., vol. 36, no. 1, pp. 64–70, 1989.
[29]. C.-L. Wei and M.-H. Shih, "Design of a Switched-Capacitor DC-DC Converter with a Wide Input Voltage Range," IEEE Trans. Circuits Syst. I Regul. Pap., vol. 60, no. 6, pp. 1648–1656, Jun. 2013.
[30]. Qing Ji, Xinbo Ruan, Ming Xu, and Fei Yang, "Effect of duty cycle on common mode conducted noise of DC-DC converters," in 2009 IEEE Energy Conversion Congress and Exposition, 2009, pp. 3616–3621.

[31]. N. Boujelben, M. Djemel and N. Derbel, "Analysis of a Quadratic Boost Converter using Sliding Mode Controller," 2020 17th International Multi-Conference on Systems, Signals & Devices (SSD), Monastir, Tunisia, 2020, pp. 969-973, doi: 10.1109/SSD49366.2020.9364205.

[32]. M. G. Ortiz-Lopez, J. Leyva-Ramos, L. H. Diaz-Saldierna, J. M. Garcia-Ibarra and E. E. Carbajal-Gutierrez, "Current-Mode Control for a Quadratic Boost Converter with a Single Switch," 2007 IEEE Power Electronics Specialists Conference, Orlando, FL, USA, 2007, pp. 2652-2657, doi: 10.1109/PESC.2007.4342436.

[33]. M. Veerachary, "Design and analysis of a new quadratic boost converter," 2017 National Power Electronics Conference (NPEC), Pune, India, 2017, pp. 307-313, doi: 10.1109/NPEC.2017.8310476.

[34]. R. V. Vamja and M. A. Mulla, "Simplified Controller Design Approach for Quadratic Boost Converter," 2018 8th IEEE India International Conference on Power Electronics (IICPE), Jaipur, India, 2018, pp. 1-6, doi: 10.1109/IICPE.2018.8709535.

[35]. S. Khursheed, K. Shi, B. M. Al-Hashimi, P. R. Wilson, and K. Chakrabarty, "Delay Test for Diagnosis of Power Switches," IEEE Trans. Very Large Scale Integr. Syst., vol. 22, no. 2, pp. 197–206, Feb. 2014.

[36]. K. D. T. Ngo and R. Webster, "Steady-state analysis and design of a switchedcapacitor DC-DC converter," IEEE Trans. Aerosp. Electron. Syst., vol. 30, no. 1, pp. 92–101, 1994.

[37]. B. Arbetter, R. Erickson, and D. Maksimovic, "DC-DC converter design for battery-operated systems," in Proceedings of PESC '95 -Power Electronics Specialist Conference, 1995, vol. 1, pp. 103–109.

[38]. K. Bhattacharyya, "Trend towards the design of embedded DC–DC converters,"IET Power Electron., vol. 6, no. 8, pp. 1563–1574, Sep. 2013.

[39]. S. V. Cheong, S. H. Chung, and A. Ioinovici, "Duty-cycle control boosts DCDC converters," IEEE Circuits Devices Mag., vol. 9, no. 2, pp. 36–37, Mar. 1993.

[40]. E. Babaei and H. M. Maheri, "Analytical Solution for Steady and Transient States of Buck DC–DC Converter in CCM," Arab. J. Sci.Eng., vol. 38, no. 12, pp.3383–3397, Jul. 2013.

[41]. T.-M. Chen and C.-L. Chen, "Analysis and design of asymmetrical half bridge flyback converter," IEE Proc. -Electr. Power Appl., vol. 149, no. 6, p. 433, 2002.

[42]. D. K. W. Cheng, "Steady-state analysis of an interleaved boost converter with coupled inductors," IEEE Trans. Ind. Electron., vol. 47, no. 4, pp. 787–795, 2000.

[43]. H. Do, "Single-Switch Buck Converter with a Ripple-Free Inductor Current,"J. Power Electron., vol. 11, no. 4, pp. 507–511, 2011.

[44]. J. C. P. Liu, N. K. Poon, B. M. H. Pong, and C. K. Tse, "Low Output Ripple DC–DC Converter Based on an Overlapping Dual Asymmetric Half-Bridge Topology," IEEE Trans. Power Electron., vol. 22, no. 5, pp. 1956–1963, Sep. 2007.

[45]. K. Bhattacharyya and P. Mandal, "Technique for the reduction of output voltage ripple of switched capacitor-based DC–DC converters," IET Circuits, Devices

Syst., vol. 5, no. 6, p. 442, 2011.
[46]. R. M. O'Connell, "On the output voltage ripple in the ideal boost and buckboost dc–dc converters," Int. J. Electron., vol. 90, no. 4, pp. 243–254, Apr. 2003.
[47]. K. C. Daly, "Ripple determination for switch-mode DC/DC converters," vol.129, no. 5. pp. 229–234, 1982.
[48]. E.H. Ismail, M. A. Al-Saffar, and A. J. Sabzali, "High Conversion Ratio DC–DC Converters With Reduced Switch Stress," IEEE Trans. Circuits Syst. I Regul. Pap., vol. 55, no. 7, pp. 2139–2151, Aug. 2008.
[49]. P. Imbertson and N. Mohan, "New directions in DC-DC power conversion based on idealized concepts leading ultimately to the asymmetrical duty-cycle power converter," IEEE Trans. Circuits Syst. I Fundam. Theory Appl., vol. 44, no. 8, pp. 722– 727, 1997.
[50]. Lung-Sheng Yang, Tsorng-Juu Liang, and Jiann-Fuh Chen, "Transformer less DC–DC Converters With High Step-Up Voltage Gain," IEEE Trans. Ind. Electron., vol. 56, no. 8, pp. 3144–3152, Aug. 2009.